




## Riboceine and N-acetylcysteine protect normal prostate cells from chemotherapy-induced oxidative stress while selectively modulating the cytotoxicity of methotrexate and docetaxel in prostate (PC-3) and breast cancer (MCF-7) cells

Trudy J. Philips<sup>a,b</sup>, Benoit Banga N'guessan<sup>a,c,d,\*</sup>, Eunice Dotse<sup>b</sup>, Joseph Kofi Abankwah<sup>a</sup>, Regina Appiah-Opong<sup>b,e,\*\*</sup> 

<sup>a</sup> Department of Pharmacology and Toxicology, School of Pharmacy, College of Health Sciences, University of Ghana, P.O. Box LG 43 Legon, Accra, Ghana

<sup>b</sup> Department of Clinical Pathology, Noguchi Memorial Institute of Medical Research, University of Ghana, P.O. Box LG 581, Accra, Ghana

<sup>c</sup> Department of Pharmacology and Toxicology, School of Pharmacy, University of Health and Allied Sciences (UHAS), PMB 31, Ho, Volta Region, Ghana

<sup>d</sup> Institute of Traditional and Alternative Medicine, University of Health and Allied Sciences (UHAS), PMB 31, Ho, Volta Region, Ghana

<sup>e</sup> Department of Biochemistry, Cell and Molecular Biology, College of Basic and Applied Sciences, University of Ghana, P.O. Box LG 71, Accra, Ghana

### ARTICLE INFO

#### Keywords:

Methotrexate  
Docetaxel  
Antioxidants  
Riboceine  
N-acetylcysteine  
Glutathione  
Reactive oxygen species

### ABSTRACT

**Background:** Cancer chemotherapy often results in severe side effects due to its non-selective cytotoxicity toward rapidly dividing normal cells. These adverse effects are largely driven by oxidative stress resulting from elevated reactive oxygen species (ROS) production. Riboceine (RIB), a synthetic precursor of glutathione (GSH), and N-acetylcysteine (NAC), a clinically used antioxidant, hold promise in mitigating oxidative damage; however, their impact on chemotherapy efficacy and the molecular mechanisms involved remain incompletely understood.

**Aim:** This study aimed to evaluate the cytoprotective potential of RIB and NAC against methotrexate (MET)- and docetaxel (DOC)-induced toxicity in normal and cancer cells, and to explore mechanistic pathways using integrative network pharmacology and molecular docking approaches.

**Methodology:** Cytotoxic effects of MET and DOC, alone or in combination with RIB or NAC, were assessed in normal prostate epithelial (PNT-2), prostate cancer (PC3), and breast cancer (MCF-7) cell lines using the Resazurin assay. Intracellular ROS and GSH levels were quantified using DCF and OPA fluorescence assays, respectively. Network pharmacology, protein-protein interaction (PPI) analysis, Gene Ontology (GO), Kyoto Encyclopedia of Genes and Genomes (KEGG) enrichment, and molecular docking were conducted using SwissTargetPrediction, STRING, ShinyGO, Cytoscape, and AutoDock Vina platforms.

**Results:** MET and DOC showed dose-dependent cytotoxicity in PNT-2 and PC3 cells, but limited efficacy in chemo-resistant MCF-7 cells. RIB and NAC significantly reduced ROS and restored GSH levels in PNT-2 cells, protecting them against oxidative injury. These antioxidants preserved anticancer effects in PC3 cells but reduced chemotherapy efficacy in MCF-7 cells, likely due to elevated redox buffering and transporter expression. Network analyses identified BCL-2, MAPK8, and SOD among key antioxidant and apoptotic targets. However, no direct experimental validation of these mechanisms was performed, and apoptotic markers such as Annexin V or caspase-3 were not assessed.

**Conclusion:** RIB and NAC provide selective cytoprotection to normal prostate cells during chemotherapy while maintaining anticancer effects in sensitive prostate cancer cells. However, their concurrent use in resistant cancers like MCF-7 may reduce drug efficacy, warranting cautious clinical application. Time-shifted antioxidant administration (e.g., post-chemotherapy) could be explored as a strategy to balance protection and efficacy. Future studies should include *in vivo* validation, apoptosis profiling, and protein-level mechanistic assays to confirm the predicted pathways.

\* Corresponding author at: Department of Pharmacology and Toxicology, School of Pharmacy, College of Health Sciences, University of Ghana, P.O. Box LG 43 Legon, Accra, Ghana.

\*\* Corresponding author at: Department of Clinical Pathology, Noguchi Memorial Institute of Medical Research, University of Ghana, P.O. Box LG 581, Accra, Ghana.

E-mail addresses: [bbnguessan@ug.edu.gh](mailto:bbnguessan@ug.edu.gh), [kbanga@uhas.edu.gh](mailto:kbanga@uhas.edu.gh) (B.B. N'guessan), [rappiah-opong@noguchi.ug.edu.gh](mailto:rappiah-opong@noguchi.ug.edu.gh) (R. Appiah-Opong).

<https://doi.org/10.1016/j.bioph.2025.118355>

Received 3 April 2025; Received in revised form 14 July 2025; Accepted 15 July 2025

Available online 20 July 2025

0753-3322/© 2025 The Author(s). Published by Elsevier Masson SAS. This is an open access article under the CC BY-NC-ND license (<http://creativecommons.org/licenses/by-nc-nd/4.0/>).

## 1. Introduction

Non-communicable diseases (NCDs), including cardiovascular diseases, asthma, stroke, diabetes, and cancer, currently account for approximately 74% of deaths worldwide, with over three-quarters of these fatalities occurring in low- and middle-income countries [1]. Among these, cancer is particularly concerning, ranking as the second leading cause of mortality globally [2]. In 2022 alone, the global burden of cancer reached 20 million new cases and approximately 9.7 million deaths, reflecting a continuous upward trend driven primarily by demographic shifts, aging populations, and lifestyle-related risk factors [3]. Projections indicate that this burden will increase further [1], underscoring the necessity for innovative approaches in cancer management, particularly in resource-limited settings.

In developing countries such as Ghana, where healthcare infrastructure and resources remain constrained, the impact of cancer is particularly severe. Recent estimates reported approximately 27,385 new cancer diagnoses and 17,944 cancer-related deaths in Ghana during 2022 [2]. Breast and cervical cancers are consistently the most prevalent among women, while liver and prostate cancers predominate among men, highlighting a critical need for improved early detection, targeted preventive strategies, and better therapeutic options [3].

The primary modalities for cancer treatment include surgery, radiotherapy, and systemic chemotherapy, the latter of which remains central due to its broad applicability in controlling tumor growth and proliferation. Chemotherapeutic agents such as methotrexate (MET) and docetaxel (DOC) disrupt cancer cell division primarily by inducing DNA damage and promoting apoptosis [4]. However, these therapies also significantly elevate the production of reactive oxygen species (ROS), leading to substantial oxidative stress in non-targeted, healthy cells [5–7]. The resulting oxidative damage contributes significantly to chemotherapy-induced toxicities, including hepatotoxicity, neurotoxicity, and myelosuppression, complicating treatment regimens and limiting therapeutic efficacy [8–11].

Reactive oxygen species, notably hydroxyl radicals ( $\text{OH}^\cdot$ ), superoxide anions ( $\text{O}_2^\cdot$ ), and hydrogen peroxide ( $\text{H}_2\text{O}_2$ ), damage critical cellular components such as lipids, proteins, and DNA, further exacerbating cellular injury [12–15]. Under normal physiological conditions, endogenous antioxidant defense systems, including glutathione (GSH), catalase, and superoxide dismutase (SOD), typically mitigate ROS-induced damage, maintaining cellular redox homeostasis [16–19]. However, during chemotherapy, the overwhelming surge in ROS production often exceeds the detoxifying capacity of these antioxidant mechanisms, resulting in oxidative stress and subsequent damage to healthy tissues [12,20].

Glutathione, the most abundant intracellular antioxidant, plays a crucial role in protecting cells from oxidative damage by scavenging ROS and facilitating detoxification processes via its cysteine residues [21–25]. Therapeutic approaches aimed at increasing GSH levels, such as the use of synthetic precursors like N-acetylcysteine (NAC) and Riboceine (RIB), have shown promise in enhancing cellular antioxidant defenses and mitigating oxidative damage during chemotherapy [26–28].

N-acetylcysteine has been extensively studied for its ability to replenish intracellular cysteine and GSH stores, thereby offering cytoprotection in various oxidative injury models, including those involving anticancer agents [26,27]. Riboceine, a novel cysteine derivative composed of D-ribose and L-cysteine, has demonstrated superior bioavailability and efficacy in elevating intracellular GSH compared to NAC in preclinical animal studies [29]. However, its potential to mitigate chemotherapy-induced cytotoxicity in human cancer and normal epithelial cells remains poorly explored, particularly in comparison with NAC.

Recent advances in cancer biology highlight the dualistic role of antioxidants during chemotherapy: while protecting healthy cells from ROS-induced toxicity, they may inadvertently shield malignant cells

from oxidative damage, potentially reducing chemotherapy efficacy [30,31]. Therefore, a critical balance must be achieved to ensure selective cytoprotection. Notably, variations in antioxidant response between cell types, such as normal epithelial cells and chemoresistant cancer cells, are often attributed to differences in redox homeostasis, transporter expression, and stress-adaptive signaling pathways [32]. These differences emphasize the importance of model selection.

MCF-7 breast cancer cell line is an established model for chemoresistant tumors due to its estrogen receptor positivity, elevated baseline antioxidant capacity, and documented overexpression of efflux proteins such as P-glycoprotein and SLC7A11 [33–35]. In contrast, PC-3 prostate cancer cells, which lack androgen receptors and exhibit greater chemosensitivity, are commonly employed to assess differential responses to chemotherapy and antioxidant co-treatment [36]. The strategic selection of these cells allows for the investigation of redox-dependent cell-type-specific responses to NAC and RIB.

ROS and GSH play a central role in chemotherapy-induced cytotoxicity, and recent studies demonstrated the pivotal role of ROS imbalance in mediating both therapeutic efficacy and off-target toxicity of anticancer agents [37,38]. Therefore, the ROS/GSH axis was selected as the primary mechanistic focus of this study, and ROS and GSH levels as reliable and mechanistically relevant approach for assessing antioxidant-mediated chemoprotection.

The aim of the present study was to investigate the chemoprotective properties of RIB and NAC against the cytotoxic effects of MET and DOC in both normal and cancer cells, focusing specifically on ROS-mediated cellular damage. Furthermore, to enhance mechanistic insight, this research employed network pharmacology and molecular docking approaches to systematically explore potential molecular targets and underlying pathways involved in the observed chemoprotective effects. These computational methods offer a cost-effective and scientifically robust alternative for generating mechanistic hypotheses, which are essential for guiding future experimental validation.

## 2. Materials and methods

### 2.1. Materials

Normal human prostate cell line; PNT-2, human prostate cancer cell line; PC3, and human breast carcinoma cell line, MCF-7 (estrogen receptor-positive) were obtained from RIKEN BioResource Center Cell Bank (Japan). Rose Park Memorial Institute (RPMI)-1640 medium, Dulbecco's Modified Eagle's Medium (DMEM), fetal bovine serum (FBS), Phosphate Buffered Saline (PBS), Trypsin, O-phthalaldehyde (OPA), Ethylenediaminetetraacetic acid (EDTA), Dimethyl Sulfoxide (DMSO), Sodium Hydroxide (NaOH), Dichlorofluorescein-Diacetate (DCF-DA), Distilled water, Resazurin, and penicillin-streptomycin antibiotic were obtained from the Clinical Pathology Department, Noguchi Memorial Institute for Medical Research (NMIMR), College of Health Sciences, University of Ghana. Riboceine was obtained from the manufacturer (Max International Ghana), NAC, and the anticancer agents (methotrexate and docetaxel) were purchased from Sigma. All reagents and chemicals were of molecular and analytical grade and obtained from standard suppliers.

### 2.2. Drug preparation

Stock solutions of MET, DOC, NAC, and RIB were prepared in DMSO. Specifically, 4.544 mg of MET and 0.808 mg of DOC were each dissolved in 1 mL DMSO to yield 10 mM and 1 mM stock solutions, respectively. NAC was prepared at 100 mM by dissolving 16.32 mg in 1 mL DMSO. For RIB, 25.33 mg was dissolved in 1 mL DMSO to yield a 100 mM stock solution, based on its molecular weight of 253.28 g/mol. All stock solutions were serially diluted with culture medium to prepare final working concentrations ranging from 0 to 10  $\mu\text{M}$  for all compounds used in the experiments.

Stock concentrations were expressed in millimolar (mM) and working concentrations were uniformly reported in micromolar ( $\mu\text{M}$ ). RIB stock solutions were freshly prepared prior to each experiment in amber vials to minimize light and air exposure. Due to the presence of a sulfur-containing moiety, RIB solutions were used promptly to prevent degradation. All stock solutions were stored at  $-20^\circ\text{C}$  until use.

### 2.3. Cell culture

The cancer cell lines PC-3 and MCF-7 were readily available in our institutional cancer cell bank and were utilized in this study. PNT-2 and PC3 cells were cultured in RPMI 1640 medium, while MCF-7 cells were cultured in DMEM medium. Both media were supplemented with 10 mM HEPES, 2 mM L-glutamine, sodium bicarbonate ( $\text{NaHCO}_3$ ), 10% FBS, and 1% penicillin-streptomycin. The cultured cells were maintained in a humidified incubator at  $37^\circ\text{C}$  with 5%  $\text{CO}_2$ . Sub-culturing was performed weekly to ensure optimal cell growth and viability.

### 2.4. Cell viability assay

The cytotoxic effects of MET and DOC, both alone and in combination with the antioxidants NAC and RIB, were evaluated using the Resazurin reduction assay, with slight modifications based on the protocol by Tsakalozou et al. [38]. Briefly, PNT-2, PC3, and MCF-7 were seeded into 96-well plates at a density of  $1 \times 10^5$  cells per well and allowed to adhere overnight at  $37^\circ\text{C}$  in a humidified incubator with 5%  $\text{CO}_2$ .

After incubation, the cells were treated with increasing concentrations of MET and DOC ranging from 0.625  $\mu\text{M}$  to 10  $\mu\text{M}$ , either alone or in combination with fixed concentrations of antioxidants. For co-treatment groups, NAC was applied at 1 mM and RIB at 3.95 mM, based on prior studies supporting their antioxidant efficacy and safety [39,40], and on preliminary data indicating optimal protective effects on PNT-2 without compromising the cytotoxic effects of MET and DOC on PC3 cells. The treatment groups included MET alone, DOC alone, RIB alone, NAC alone, MET+RIB, MET+NAC, DOC+RIB, and DOC+NAC.

After 24 h of treatment, 10  $\mu\text{L}$  of Resazurin solution (0.15 mg/mL in PBS) was added to each well, followed by a 4-hour incubation at  $37^\circ\text{C}$ . The 24-hour exposure duration was selected based on literature evidence indicating peak uptake of chemotherapeutic agents and significant oxidative stress induction within this time frame [41]. Fluorescence intensity was then measured using a Tecan Infinite M200 microplate reader (Austria) with excitation and emission wavelengths of 560 nm and 590 nm, respectively. All treatments were conducted in triplicate across three independent experiments.

To quantify the cytotoxicity of MET and DOC, concentration-response curves were generated and half-maximal inhibitory concentration ( $\text{IC}_{50}$ ) values were calculated for each drug in all three cell lines. From these, selectivity indices (SI) were determined by comparing  $\text{IC}_{50}$  values in normal versus cancer cell lines. Additionally, area under the curve (AUC) analyses were used to quantitatively compare treatment efficacy across the full concentration range.

### 2.5. Glutathione assay

The GSH levels in the cells were quantified using the orthophthalaldehyde (OPA) assay, as described by Martín et al. [42]. Cultured cells were seeded at a density of  $2 \times 10^5$  cells per well in a 24-well plate and incubated overnight at  $37^\circ\text{C}$  in a humidified atmosphere with 5%  $\text{CO}_2$ . After incubation, the cells were treated with MET, DOC, RIB, NAC (positive control), or hydrogen peroxide ( $\text{H}_2\text{O}_2$ , negative control) at varying concentrations. Additionally, combinations of MET or DOC or  $\text{H}_2\text{O}_2$  with RIB or NAC were tested (i.e., MET+RIB, MET+NAC, DOC+RIB, DOC+NAC,  $\text{H}_2\text{O}_2$ +RIB, and  $\text{H}_2\text{O}_2$ +NAC).

Following 24 h of treatment, the cells were detached and homogenized by ultrasonication in 5% trichloroacetic acid containing 2 mM EDTA for 15 min. The homogenates were centrifuged at 3000 rpm for

30 min (Hettich Zentrifugen MIKRO 200, Germany). A 50  $\mu\text{L}$  aliquot of the resulting supernatant was transferred to a 96-well plate, neutralized by adding 10  $\mu\text{L}$  of 1 M sodium hydroxide (NaOH), and further mixed with 50  $\mu\text{L}$  of sodium phosphate buffer. Subsequently, 10  $\mu\text{L}$  of OPA solution (10 mg/mL) was added, and the plate was incubated in the dark at room temperature ( $26^\circ\text{C}$ ) for 15 min. The GSH levels in the supernatant were determined by measuring fluorescence with an excitation wavelength of 340 nm and an emission wavelength of 460 nm.

### 2.6. Measurement of intracellular reactive oxygen species

The intracellular ROS levels were measured using the dichlorofluorescein (DCF) assay, as described by Kawiak et al. [43]. Cultured cells were seeded in a 24-well plate at a density of  $2 \times 10^5$  cells per well and incubated overnight at  $37^\circ\text{C}$  in a humidified atmosphere containing 5%  $\text{CO}_2$ . Following incubation, the spent media was discarded and replaced with serum-free media. The cells were then treated with varying concentrations of MET, DOC, RIB, NAC, and their combinations (MET+NAC, MET+RIB, DOC+NAC, and DOC+RIB).

After 24 h of treatment, 10  $\mu\text{L}$  of 5  $\mu\text{M}$  2',7'-dichlorofluorescein diacetate (DCFDA) was added to each well, and the plates were incubated for an additional 120 min. The fluorescence intensity, indicative of intracellular ROS levels, was measured at an excitation wavelength of 485 nm and an emission wavelength of 530 nm.

### 2.7. Screening of potential targets and intersection analysis

Potential molecular targets related to breast cancer, prostate cancer, and oxidative stress were screened using the GeneCards database (<https://www.genecards.org/>) and the Online Mendelian Inheritance in Man (OMIM) database. A relevance score threshold greater than 10 was applied in GeneCards to ensure the selection of highly relevant gene targets associated with each disease and oxidative stress condition [44]. Additionally, the molecular targets of docetaxel (DOC), methotrexate (MET), ribocicline (RIB), and N-acetylcysteine (NAC) were obtained from the SwissTargetPrediction database. Venn diagrams illustrating intersecting molecular targets among prostate cancer, oxidative stress, and antioxidant treatments were generated using an online bioinformatics tool available at <http://www.bioinformatics.com.cn>. Furthermore, common targets among oxidative stress, chemotherapeutic drugs (DOC and MET), and cancer types (breast and prostate cancers) were visualized and analyzed using Cytoscape software (version 3.7.2).

### 2.8. Construction of protein-protein interaction (PPI) network and identification of core targets

Common molecular targets were imported into the STRING database (<https://cn.string-db.org/>) to construct protein-protein interaction (PPI) networks. Parameters were set for Homo sapiens, with interactions having a confidence score threshold of 0.7 considered significant to ensure the robustness of the predicted interactions [45]. Disconnected nodes were removed to refine network visualization. Subsequently, the refined PPI network was imported into Cytoscape (version 3.7.2) for visualization and further topological analysis. Using the CytoHubba plugin, the top 10 hub targets were identified based on the Maximal Clique Centrality (MCC) algorithm, a method that emphasizes densely interconnected nodes and their biological relevance within the network.

### 2.9. GO functional enrichment and KEGG pathway analysis

To elucidate the biological significance of the identified hub targets, Gene Ontology (GO) functional enrichment and Kyoto Encyclopedia of Genes and Genomes (KEGG) pathway enrichment analyses were performed using the ShinyGO database. The analysis focused on the top 10 key targets identified from the PPI network, setting the organism parameter to *Homo sapiens* and a statistical significance threshold of

$p < 0.05$ . The top 20 enriched signaling pathways were determined, along with the top 10 most significant terms for each of the GO categories: Molecular Functions (MF), Cellular Components (CC), and Biological Processes (BP).

2.10. Molecular docking validation of core targets

Molecular docking analyses were performed to validate the predicted interactions between identified targets and selected small molecules.

Molecular docking is commonly utilized in drug discovery to evaluate the potential binding affinity between ligands (small molecules) and protein receptors. Docking affinity is typically reported as negative energy values (kcal/mol), with lower values indicating stronger and more favorable ligand-protein interactions [46]. In this study, the 3D structures of key target proteins identified through network pharmacology were retrieved from the Protein Data Bank (<https://www.rcsb.org/>). Similarly, 3D structures of ligands, ribocicaine, N-acetylcysteine, methotrexate, and docetaxel, were obtained from the PubChem database (<http://pubchem.ncbi.nlm.nih.gov/>)

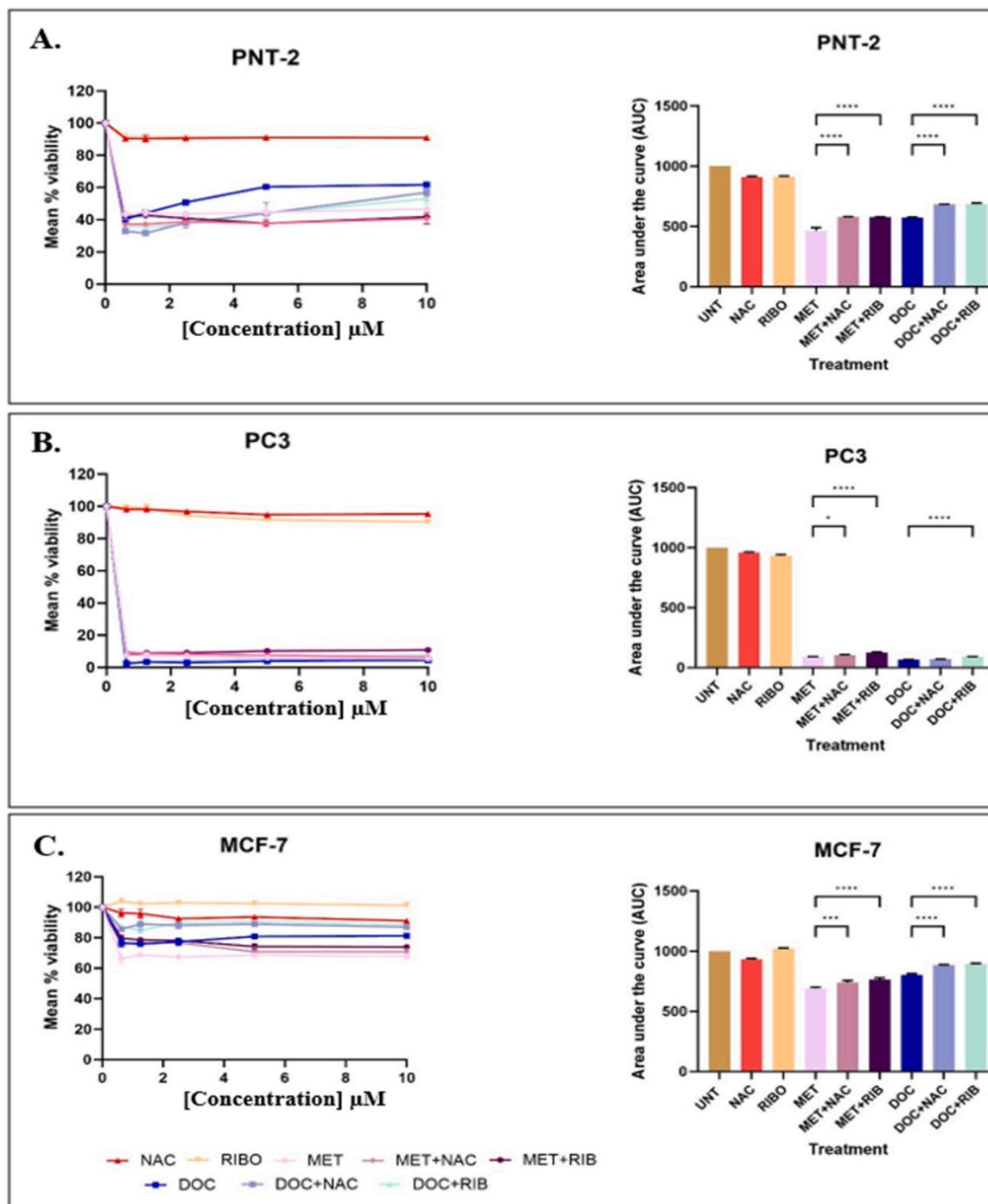


**Fig. 1.** The concentration-response curve and their area under the curve of (A) Cytoprotective effects of RIB and NAC against the cytotoxic activity of MET and DOC on PNT-2, (B) The preservation of the cytotoxic activity of MET and DOC against PC3 in the presence of RIB and NAC and (C) The impairment of the cytotoxicity of MET and DOC against MCF-7 cells in the presence of RIB and NAC. Data are means  $\pm$  SEM (n = 3). Statistical significance by student's t-test; P values  $\leq 0.05$ ,  $\leq 0.02$  and  $\leq 0.001$  and are denoted by the symbols \*, \*\* and \*\*\* respectively. ROS- Reactive Oxygen Species; MET- Methotrexate; DOC- Docetaxel; RIB- Ribocicaine; NAC- N-acetylcysteine.

ps://pubchem.ncbi.nlm.nih.gov). PyMOL software (version 2.5) was utilized for the preparation of ligands and receptor proteins, involving the removal of water molecules, non-participating side chains, and existing ligands where necessary. Molecular docking simulations were conducted using AutoDock Vina software, and the results were visualized with PyMOL 2.5. Specifically, superoxide dismutase (SOD, PDB ID: 1PUO) [47] was docked with ribocele, while protein tyrosine phosphatase 1B (PTPN1, PDB ID: 1ONZ) [48]. was docked with NAC. Additionally, proteins with MCC scores above 190, Bcl-2 (PDB ID: 2W3L) [48], and MAPK8 (PDB ID: 2XRW) [49] were docked with docetaxel, whereas the folate receptor alpha (FOLR1, PDB ID: 4LRH) [50] was docked with methotrexate.

### 2.11. Statistical analysis

The results are expressed as the mean  $\pm$  standard deviation (SD) from three independent experiments. Percentage inhibition was calculated as the ratio of the activity of treated samples to that of the control samples. Half-maximal inhibitory concentration ( $IC_{50}$ ) values were determined using GraphPad Prism software. Statistical comparisons were performed using the Student's *t*-test for two-group comparisons and one-way analysis of variance (ANOVA) for multiple-group analyses. A *p*-value less than 0.05 ( $p < 0.05$ ) was considered statistically significant.

## 3. Results

### 3.1. Cytoprotective effects of ribocele and N-acetylcysteine against methotrexate- and docetaxel-induced cytotoxicity in normal and cancer cells

The results demonstrate the cytoprotective effects of RIB and NAC against the cytotoxic activities of MET and DOC on PNT-2, PC3, and MCF-7 cells. As shown in Fig. 1, RIB and NAC significantly enhanced cell viability, particularly in normal cells (PNT-2), suggesting their potential in mitigating the toxic effects of chemotherapy. The area under the curve (AUC) values further quantified the extent of this cytoprotection. For PNT-2 cells treated with MET, co-treatment with RIB or NAC showed statistical significance at  $p \leq 0.001$  compared to MET alone, while for DOC-treated PNT-2 cells, co-treatment with RIB or NAC was significant at  $p \leq 0.02$ . In PC3 cells, the addition of RIB or NAC significantly improved cell viability at  $p \leq 0.05$  in both MET- and DOC-treated groups. No statistically significant cytoprotection was observed for MCF-7 cells under similar conditions.

Additionally, the  $IC_{50}$  values presented in Table 1 revealed that MET and DOC exhibited greater potency against PC3 cells (prostate cancer) compared to PNT-2 (normal cells), with  $IC_{50}$  values of  $0.338 \pm 0.001 \mu\text{M}$  and  $0.320 \pm 0.001 \mu\text{M}$ , respectively, versus  $0.552 \pm 0.029 \mu\text{M}$  and  $0.524 \pm 0.010 \mu\text{M}$  for PNT-2 cells. In contrast, the  $IC_{50}$  values for MCF-7 cells (breast cancer) exceed  $10 \mu\text{M}$  for both MET and DOC, indicating reduced sensitivity to these drugs. The selective index (SI) values further highlight the limited selectivity of MET and DOC toward MCF-7 cells, with values of 0.055 and 0.052, respectively, compared to PC3 cells, which exhibit higher SI values of 1.633 and 1.638.

These findings underscore the efficacy of RIB and NAC in protecting normal cells from chemotherapy-induced damage while maintaining

**Table 1**

Inhibitory concentration fifty ( $IC_{50}$ ) and selective index (SI) values of MET and DOC on PNT-2, PC3 and MCF-7 Cells.

DRUGS CELLS	$IC_{50}$ Values ( $\mu\text{M}$ )		Selective Index (SI)	
	MET	DOC	MET	DOC
PNT-2	$0.552 \pm 0.029$	$0.524 \pm 0.010$	-	-
PC3	$0.338 \pm 0.001$	$0.320 \pm 0.001$	1.633	1.638
MCF-7	> 10	> 10	0.055	0.052

Data are means  $\pm$  SEM (n = 3)

some selective cytotoxicity against prostate cancer cells. However, the low selectivity for MCF-7 cells raises concerns about the broader applicability of MET and DOC in breast cancer treatment, emphasizing the need for additional strategies to enhance therapeutic selectivity and efficacy.

### 3.2. Effects of ribocele and N-acetylcysteine on glutathione levels in normal and cancer cells treated with methotrexate and docetaxel

The results presented in Fig. 2 illustrate the effects of NAC, RIB, hydrogen peroxide ( $\text{H}_2\text{O}_2$ ), MET, DOC, and their combinations on GSH content in PNT-2, PC3, and MCF-7 cells.

In PNT-2 cells (Fig. 2A), both NAC and RIB significantly increased GSH levels compared to untreated (UNT) cells ( $p \leq 0.001$ ). Treatment with MET or DOC alone significantly reduced GSH levels ( $p \leq 0.001$ ) compared to UNT cells. However, the addition of NAC or RIB to MET (MET+NAC, MET+RIB) or DOC (DOC+NAC, DOC+RIB) significantly restored GSH levels. Specifically, co-treatment with NAC resulted in significant differences compared to MET ( $p \leq 0.05$ ) and DOC ( $p \leq 0.05$ ), while co-treatment with RIB similarly restored GSH with significant differences compared to MET ( $p \leq 0.05$ ) and DOC ( $p \leq 0.05$ ).

In PC3 cells (Fig. 2B), NAC and RIB also significantly elevated GSH levels compared to UNT cells ( $p \leq 0.001$ ). Treatment with MET or DOC alone significantly reduced GSH content ( $p \leq 0.001$ ). Co-treatment with NAC or RIB significantly mitigated these reductions, with NAC showing significant differences compared to MET ( $p \leq 0.05$ ) and DOC ( $p \leq 0.05$ ), and RIB showing similar significant differences compared to MET ( $p \leq 0.05$ ) and DOC ( $p \leq 0.05$ ).

In MCF-7 cells (Fig. 2C), the effects were less pronounced. NAC and RIB slightly increased GSH levels compared to UNT cells, though the increases were not as substantial as in PNT-2 or PC3 cells. MET and DOC treatments significantly reduced GSH levels ( $p \leq 0.001$ ), and the addition of NAC or RIB provided some restoration of GSH levels. However, the restoration was less significant in MCF-7 cells, with co-treatment showing only partial mitigation.

These results indicate that RIB and NAC significantly enhance GSH levels, thereby mitigating the oxidative damage caused by MET and DOC. The protective effects were most notable in normal cells (PNT-2) and prostate cancer cells (PC3), while MCF-7 cells exhibited limited responses, suggesting cell-line-specific differences in GSH metabolism. This highlights the potential of NAC and RIB as adjuncts to chemotherapy, particularly for reducing oxidative stress in normal and prostate cancer cells.

### 3.3. Effects of ribocele and N-acetylcysteine on chemotherapy-induced oxidative stress in normal and cancer cell lines

The results in Table 2 present the effects of MET, DOC, NAC, RIB, and their combinations on ROS levels, measured as mean intensity fluorescence (MIF), in PNT-2, PC3, and MCF-7 cells.

In PNT-2 cells (normal cells), UNT cells exhibited baseline ROS levels of  $6795.5 \pm 30.41$ . Treatment with MET and DOC significantly increased ROS levels to  $8639 \pm 530.33$  ( $p \leq 0.05$ ) and  $7584 \pm 49.50$  ( $p \leq 0.02$ ), respectively. NAC and RIB treatments alone significantly reduced ROS levels compared to UNT cells, with ROS levels decreasing to  $4445.5 \pm 147.79$  ( $p \leq 0.02$ ) and  $4892.5 \pm 65.76$  ( $p \leq 0.001$ ), respectively. The combination of MET with NAC (MET+NAC) and MET with RIB (MET+RIB) significantly reduced ROS levels compared to MET alone, with ROS levels of  $5760.5 \pm 263.75$  ( $p \leq 0.05$ ) and  $5582.5 \pm 768.63$  ( $p \leq 0.05$ ), respectively. Similarly, DOC combinations with NAC (DOC+NAC) and RIB (DOC+RIB) further reduced ROS levels to  $5499 \pm 346.48$  ( $p \leq 0.05$ ) and  $4721 \pm 45.25$  ( $p \leq 0.001$ ), respectively.

In PC3 cells, untreated cells exhibited baseline ROS levels of  $5645 \pm 137.18$ . MET and DOC treatments increased ROS levels to  $6360 \pm 241.83$  and  $5914.5 \pm 28.99$ , respectively, though the increase was not as pronounced as in PNT-2 cells. NAC and RIB treatments alone reduced

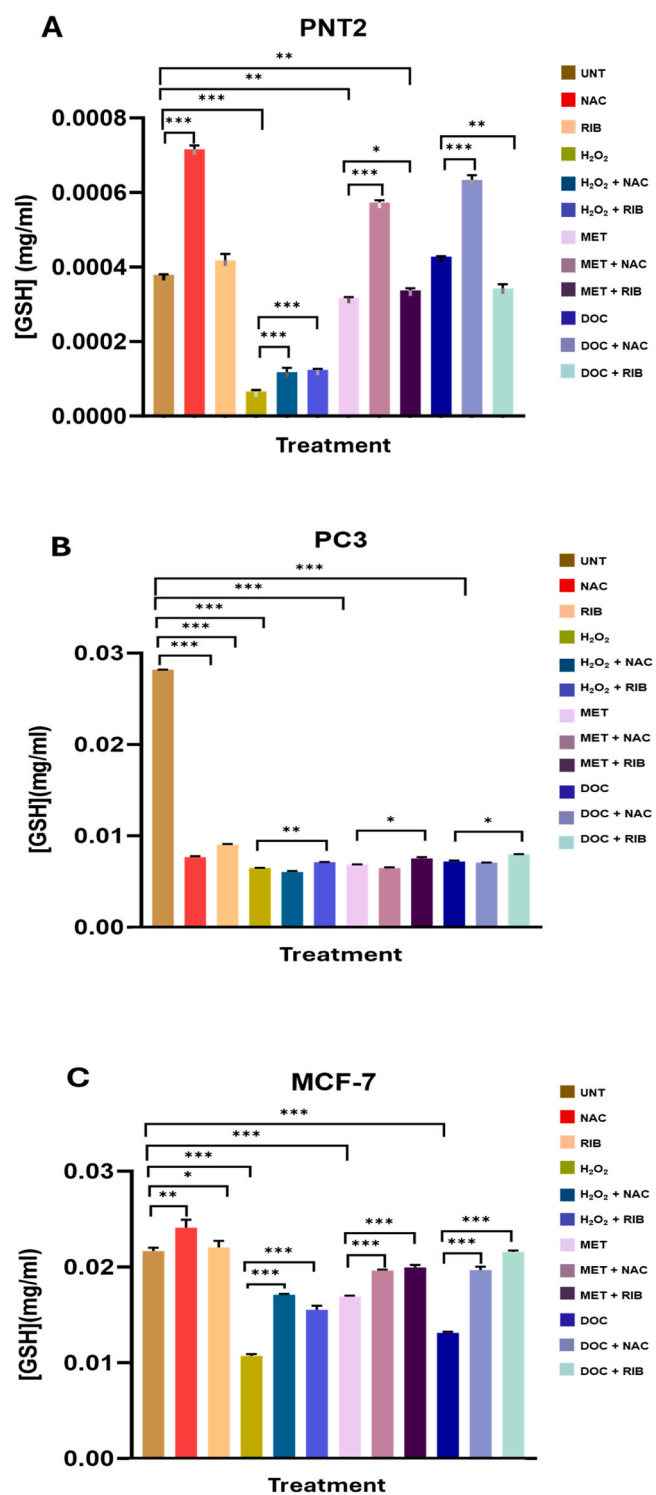


**Fig. 2.** Effects of N-acetylcysteine, Ribocaine, Hydrogen peroxide, Methotrexate, Docetaxel and their combinations on GSH content of (A) PNT-2, (B) PC3 and (C) MCF-7 cells. Data are means  $\pm$  SEM (n = 3). Statistical significance by student's *t*-test; P values  $\leq$  0.05,  $\leq$  0.02 and  $\leq$  0.001 and are denoted by the symbols \*, \*\* and \*\*\* respectively when compared to the untreated (UNT) cells. The symbol # denotes comparison between MET vs MET+NAC or DOC vs DOC+NAC, \$ denotes comparison between MET vs MET+RIB and DOC vs DOC+RIB. ROS- Reactive Oxygen Species. MET- Methotrexate DOC- Docetaxel RIB- Ribocaine NAC- N-acetylcysteine.

**Table 2**

Effects of methotrexate (MET), docetaxel (DOC), N-acetylcysteine (NAC), ribocaine (RIB) and their combination on ROS level of PNT-2, PC3 and MCF-7 cells.

Treatment	ROS Level (MIF)		
	PNT- 2	PC3	MCF-7
UNT	6795.5 $\pm$ 30.41	5645 $\pm$ 137.18	16419.5 $\pm$ 44.55
MET	8639 $\pm$ 530.33*	6360 $\pm$ 241.83	14858 $\pm$ 19.80***
DOC	7584 $\pm$ 49.50**	5914.5 $\pm$ 28.99	13500 $\pm$ 308.30**
NAC	4445.5 $\pm$ 147.79**	4908 $\pm$ 106.77*	10736 $\pm$ 104.65***
RIB	4892.5 $\pm$ 65.76***	4793.5 $\pm$ 104.65*	11818 $\pm$ 132.94***
MET+NAC	5760.5 $\pm$ 263.75*#†	5960 $\pm$ 209.30 <sup>†</sup>	13138 $\pm$ 209.30***#††
MET+RIB	5582.5 $\pm$ 768.63 <sup>§</sup>	6007.5 $\pm$ 225.57 <sup>‡</sup>	14634.5 $\pm$ 36.06***§§††
DOC+NAC	5499 $\pm$ 346.48*#	5790 $\pm$ 195.16 <sup>†</sup>	12013.5 $\pm$ 215.67**#†
DOC+RIB	4721 $\pm$ 45.25***§§§	5966.5 $\pm$ 243.95 <sup>‡</sup>	12595 $\pm$ 312.54**

Data are means  $\pm$  SEM (n = 3). Statistical significance by student's *t*-test; P values  $\leq$  0.05,  $\leq$  0.02 and  $\leq$  0.001 and are denoted by the symbols \*, \*\* and \*\*\* respectively when compared to the untreated (UNT) cells. The symbol # denotes comparison between MET vs MET+NAC or DOC vs DOC+NAC, \$ denotes comparison between MET vs MET+RIB and DOC vs DOC+RIB, † denotes NAC vs MET+NAC and NAC vs DOC+NAC and ‡ denotes RIB vs MET+RIB and RIB vs DOC+RIB. ROS- Reactive Oxygen Species. MET- Methotrexate DOC- Docetaxel, RIB- Ribocaine, NAC- N-acetylcysteine

ROS levels significantly to 4908  $\pm$  106.77 ( $p \leq$  0.05) and 4793.5  $\pm$  104.65 ( $p \leq$  0.05), respectively. The combination treatments MET+NAC and MET+RIB resulted in ROS levels of 5960  $\pm$  209.30 and 6007.5  $\pm$  225.57, showing modest reductions compared to MET alone. DOC combinations with NAC and RIB reduced ROS levels to 5790  $\pm$  195.16 and 5966.5  $\pm$  243.95, with varying degrees of statistical significance.

In MCF-7 cells, untreated cells showed higher baseline ROS levels of 16419.5  $\pm$  44.55. Treatment with MET and DOC resulted in reduced ROS levels of 14858  $\pm$  19.80 ( $p \leq$  0.001) and 13500  $\pm$  308.30 ( $p \leq$  0.02), respectively. NAC and RIB treatments significantly reduced ROS levels to 10736  $\pm$  104.65 ( $p \leq$  0.001) and 11818  $\pm$  132.94 ( $p \leq$  0.001). The combination treatments MET+NAC and MET+RIB resulted in ROS levels of 13138  $\pm$  209.30 ( $p \leq$  0.02) and 14634.5  $\pm$  36.06 ( $p \leq$  0.001), respectively. DOC combinations with NAC and RIB resulted in further reductions in ROS levels to 12013.5  $\pm$  215.67 ( $p \leq$  0.02) and 12595  $\pm$  312.54 ( $p \leq$  0.02), respectively.

These results highlight the ability of NAC and RIB to reduce ROS levels, both as standalone treatments and in combination with MET and DOC. The effects were most pronounced in normal PNT-2 cells, with notable reductions also observed in PC3 cells. However, ROS reductions in MCF-7 cells were less pronounced, suggesting cell-line-specific differences in the response to oxidative stress.

#### 3.4. Identification of common core targets and protein-protein interaction (PPI) Network

Potential molecular targets associated with the anticancer drugs (DOC and MET), antioxidants (NAC and RIB), oxidative stress, and the selected cancers (prostate and breast) were systematically identified through network pharmacology analysis (Fig. 3A). Initial screening revealed a total of 28 overlapping targets common to prostate cancer, oxidative stress, and the anticancer agents, which also intersected significantly with targets identified for breast cancer, oxidative stress, and anticancer agents (Fig. 3B). Further detailed evaluation demonstrated that DOC was associated with all 28 identified targets, indicating its broad interaction profile; however, MET showed a much narrower target association, overlapping with only one of these targets (Fig. 3C). On the other hand, NAC exhibited multiple overlapping targets with breast cancer, prostate cancer, and oxidative stress, highlighting its potential to modulate multiple oxidative stress-related pathways (Fig. 3D).

To visualize these intricate interactions, a comprehensive drug-target-disease network was constructed using Cytoscape software



(Fig. 3E). Subsequent refinement by applying stringent high-confidence interaction criteria (confidence score > 0.7) using the STRING database resulted in a final PPI network comprising 22 intersecting target proteins (Figure 43 F). Topological analysis of this network using the CytoHubba plugin and the Maximal Clique Centrality (MCC) algorithm identified ten hub proteins of critical biological significance: BCL2, MAPK8, TNF, MAPK14, MAPK1, MAP2K1, EGFR, MMP9, MAPK9, and HSP90AB1 (Fig. 3G).

### 3.5. Kyoto encyclopedia of genes and genomes (KEGG) and gene ontology (GO) enrichment analysis

KEGG pathway analysis identified significant enrichment of the identified targets in several cancer-related and oxidative stress-associated signaling pathways. Among the top 20 significantly enriched pathways ( $p < 0.05$ ), endocrine resistance, relaxin signaling, hepatitis, colorectal cancer, lipid metabolism and atherosclerosis, IL-17 signaling, GnRH signaling, and prostate cancer signaling pathways were notably prominent (Fig. 4A). In particular, the prostate cancer-associated pathways encompassed pivotal cellular processes such as the PI3K-Akt signaling pathway, p53 signaling pathway, and the MAPK signaling pathway (Fig. 4B).

Gene Ontology (GO) functional enrichment further categorized the top 10 enriched terms into three categories: biological processes (BP), cellular components (CC), and molecular functions (MF). The BP category prominently featured cellular response to cadmium ions, responses to reactive oxygen species, stress-activated MAPK cascade, stress-activated protein kinase signaling cascade, and peptidyl-serine phosphorylation. The CC terms highlighted included ooplasm, Ficolin-1-rich granule lumen, Ficolin-1-rich granules, vesicle lumen, and late endosomes. Molecular function (MF) analysis indicated enrichment of JUN kinase activity, nitric oxide synthase regulator activity, MAP kinase activity, MAP kinase kinase activity, and protein phosphatase binding (Fig. 4C).

### 3.6. Molecular docking validation of key compound-target interactions

Molecular docking was utilized to validate and evaluate predicted interactions between identified core target proteins and relevant bioactive compounds presented in Fig. 5. The docking analysis demonstrated strong binding affinities for DOC with BCL2 (Fig. 6A, binding energy:  $-7.91$  kcal/mol) and MAPK8 (Fig. 6B, binding energy:  $-6.21$  kcal/mol). MET exhibited a particularly high binding affinity toward FOLR1 with a binding energy of  $-9.7$  kcal/mol (Fig. 6C). Similarly, RIB showed effective interaction with SOD, displaying a binding energy of  $-5.31$  kcal/mol (Fig. 6D). NAC presented a modest interaction affinity with PTPN1, exhibiting a binding energy of  $-4.4$  kcal/mol.

Further visualization and analysis of these docking interactions using PyMOL revealed distinct interaction profiles. DOC formed robust hydrogen bond networks with BCL2 residues ARG-105, GLU-95, and VAL-92, and extensive hydrogen bonding interactions with MAPK8 residues GLY-35, GLY-38, SER-34, GLY-33, VAL-40, SER-155, and ASN-114. MET exhibited strong electrostatic interactions and hydrogen bonds with FOLR1 residues ASP-81, THR-82, and SER-174. Likewise, the antioxidant RIB formed a stable complex with SOD, mediated through hydrogen bonds with residues LYS-70, HIS-80, ASN-65, HIS-63, THR-135, and GLU-132. These results confirm favorable binding interactions, supporting their mechanistic roles in modulating oxidative stress and cancer-related pathways.

## 4. Discussion

Cancer chemotherapy is frequently accompanied by serious limitations, including the development of drug resistance and adverse effects on healthy tissues. A critical drawback of conventional chemotherapeutic agents such as methotrexate (MET) and docetaxel (DOC) is their lack of selectivity, resulting in cytotoxic damage not only to cancer cells

but also to rapidly proliferating normal cells. These toxic effects are largely associated with increased intracellular generation of reactive oxygen species (ROS), which disrupt redox homeostasis and damage essential biomolecules. In the present study, we evaluated the cytoprotective potential of D-ribose-L-cysteine (RIB), a synthetic precursor for glutathione (GSH) biosynthesis, in normal and cancer cell lines exposed to MET and DOC. We also investigated whether co-treatment with RIB or the widely used antioxidant N-acetylcysteine (NAC) would compromise the anticancer efficacy of these drugs. While mechanistic assays were not performed in this study, we complemented our *in vitro* findings with computational analyses to provide mechanistic insight. Specifically, we employed an integrative network pharmacology and molecular docking approach to predict potential molecular targets and pathways modulated by the chemotherapeutic agents and antioxidants. This dual approach allowed to explore the therapeutic potential of NAC and RIB while acknowledging the need for future experimental validation.

The Resazurin assay confirmed the dose-dependent cytotoxic effects of MET and DOC on PNT-2 cells (normal prostate epithelial cells), highlighting their lack of selectivity and potential for off-target toxicity in non-malignant tissues. Notably, co-treatment with RIB or NAC significantly reduced the cytotoxic effects of MET and DOC on PNT-2 cells, demonstrating their potential cytoprotective roles. This observation is consistent with previous studies showing that NAC attenuates cisplatin-induced oxidative damage in non-cancerous cells through GSH replenishment and ROS scavenging [51]. In contrast, MET and DOC exerted stronger cytotoxic effects on PC3 cells (prostate cancer cells), and co-treatment with RIB or NAC did not rescue cell viability, suggesting selective preservation of chemotherapy efficacy in malignant cells. This could be attributed to the preferential uptake of MET through folate transport systems, such as the reduced folate carrier (RFC) and folate receptors, which are upregulated in many tumors [52]. Similarly, DOC-induced apoptosis in PC3 cells has been linked to microtubule stabilization and phosphorylation of pro-apoptotic proteins such as Bcl-2 [38]. However, it has also been reported that NAC may, under certain conditions, reduce docetaxel sensitivity in prostate cancer cells by modulating ROS-mediated apoptosis signaling [53,54], indicating that antioxidant effects may vary depending on cellular context, drug concentration, or timing of administration.

In contrast, MCF-7 breast cancer cells exhibited resistance to both MET and DOC, consistent with reports of overexpression of efflux proteins, including breast cancer resistance protein (BCRP) and multidrug resistance proteins (MRP1 and MRP5), which limit intracellular drug accumulation and reduce cytotoxic efficacy [55]. Furthermore, modifications in microtubule-associated proteins (MAPs), overexpression of class III  $\beta$ -tubulin isoforms, and altered apoptotic signaling pathways in MCF-7 cells have been implicated in DOC resistance [56,57]. Co-treatment with RIB or NAC partially restored cell viability in MCF-7 cells treated with MET or DOC, suggesting a potential unintended protective effect of these antioxidants on drug-resistant breast cancer cells. This finding aligns with previous studies, such as those by Sahin et al. [58], which reported reduced MET-induced cytotoxicity in leukemia cells following antioxidant supplementation. Such antioxidant-induced chemoprotection may be attributed to enhanced redox buffering, modulation of apoptosis regulators, or modulation of transporter-related and metabolic pathways. Notably, NAC has been shown to interfere with chemotherapeutic efficacy by altering cellular uptake, inducing phase II metabolic enzymes, upregulating efflux transporters such as P-glycoprotein (P-gp) and ABCG2, or elevating intracellular GSH levels, thereby mitigating ROS-induced cytotoxicity [53,59]. These interactions are illustrated in Fig. 7, which depicts how NAC and RIB may enhance antioxidant defense and indirectly support drug efflux mechanisms via SLC7A11 and redox-sensitive signaling. These findings underscore the importance of timing and dosage when using antioxidants during chemotherapy, particularly in resistant cancers like MCF-7, where antioxidant co-treatment may compromise therapeutic efficacy.

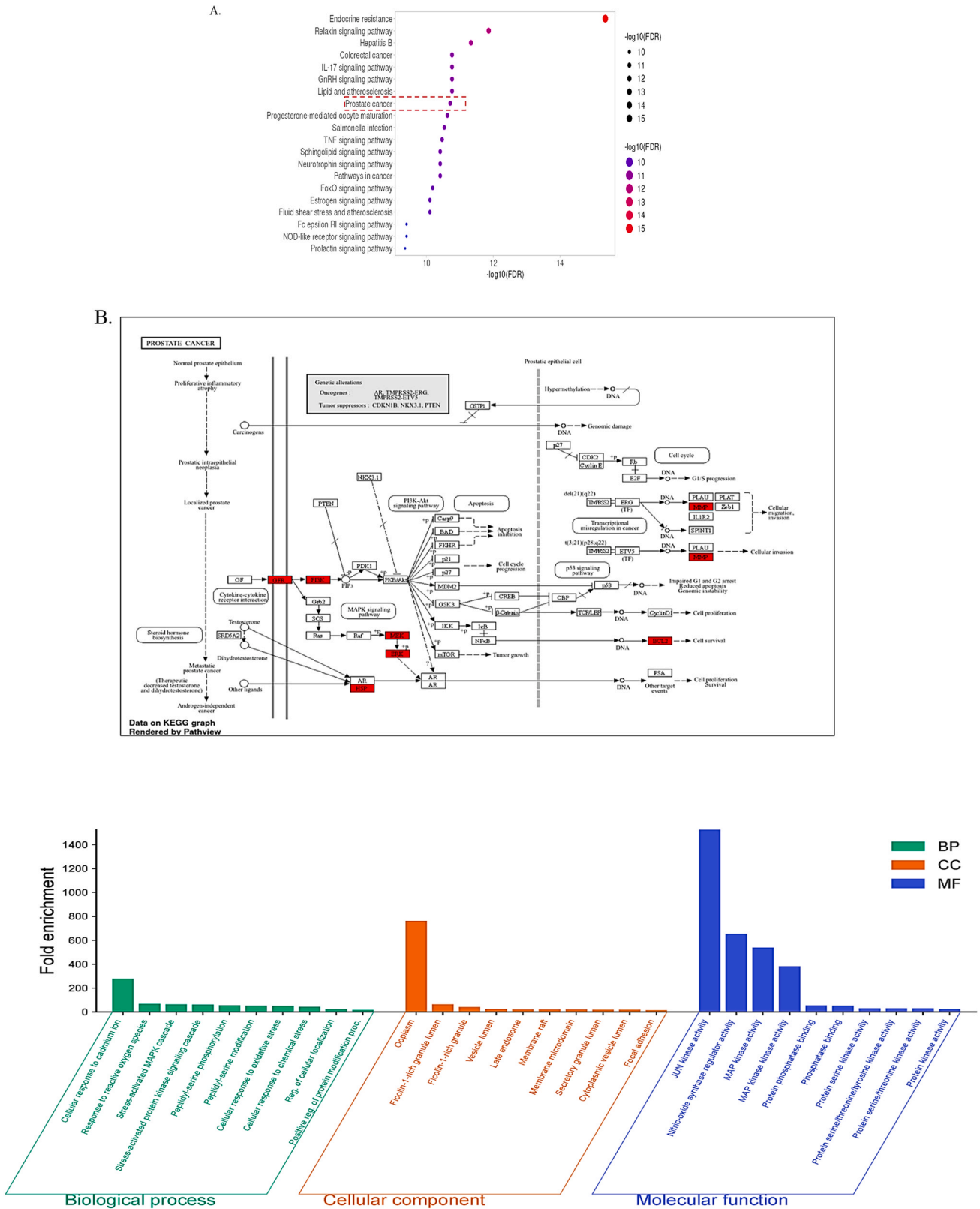


**Fig. 4.** Bioinformatic analysis of the common top 10 key targets. (A) KEGG pathway enrichment analysis showing the top 20 signaling pathways associated with the core targets identified through network pharmacology. (B) Detailed KEGG pathway map highlighting the involvement of core targets in the prostate cancer pathway, illustrating their functional roles in tumor progression and therapeutic modulation. (C) Gene Ontology (GO) enrichment analysis of the top 10 terms in three categories: biological process (BP), cellular component (CC), and molecular function (MF).

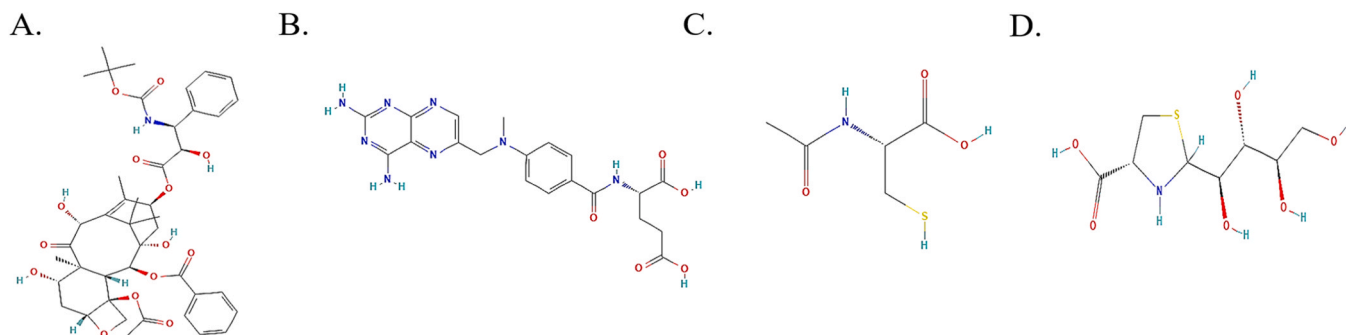


**Fig. 5.** Chemical structures of docetaxel (A), methotrexate (B), N-acetylcysteine (C), and riboceine (D). The 2D structural diagrams of the four compounds were retrieved from the PubChem database. These structures were used for subsequent molecular docking analyses to explore their interactions with core protein targets identified through network pharmacology.

GSH assays revealed that MET significantly depleted GSH levels in PNT-2 cells, potentially due to its inhibitory effects on dihydrofolate reductase (DHFR) and subsequent depletion of NADPH, a critical cofactor for GSH regeneration, thereby leading to increased ROS generation [60]. Conversely, DOC treatment increased GSH content in PNT-2 cells, likely as a compensatory antioxidant response to DOC-induced oxidative stress. NAC effectively restored GSH levels in PNT-2 cells by supplying cysteine, the rate-limiting substrate for GSH biosynthesis via the  $\gamma$ -glutamyl cycle. RIB also restored GSH levels but to a lesser extent, possibly due to a slower enzymatic release of L-cysteine from the ribose-cysteine complex or limited uptake through cysteine transporters. This observation is supported by previous findings that RIB increases GSH levels, glutathione peroxidase (GPx) activity, and superoxide dismutase (SOD) activity in diabetic mice [61]. Combined treatment with MET or DOC and either RIB or NAC further increased GSH content in PNT-2 cells, reinforcing the role of these antioxidants in

protecting normal cells from chemotherapy-induced oxidative stress. Cancer cells, particularly untreated MCF-7 cells, exhibited elevated baseline GSH levels compared to PNT-2 cells, a phenomenon often associated with reduced oxidative stress, enhanced resistance to apoptosis, and increased drug resistance [25]. MET and DOC treatment depleted GSH in PC3 and MCF-7 cells, increasing their susceptibility to oxidative stress and enhancing drug-induced cytotoxicity.

ROS assays confirmed that untreated cancer cells (PC3 and MCF-7) exhibited higher ROS levels than PNT-2 cells, reflecting the heightened oxidative stress in cancer cells due to increased metabolic activity and oncogenic transformations [62]. Treatment with NAC and RIB significantly reduced ROS levels across all cell lines, which can be attributed to their well-established roles as GSH precursors and ROS scavengers. Importantly, RIB and NAC reduced ROS levels in PNT-2 cells while preserving the cytotoxic effects of MET and DOC on PC3 cells, suggesting that redox modulation by these antioxidants did not impair

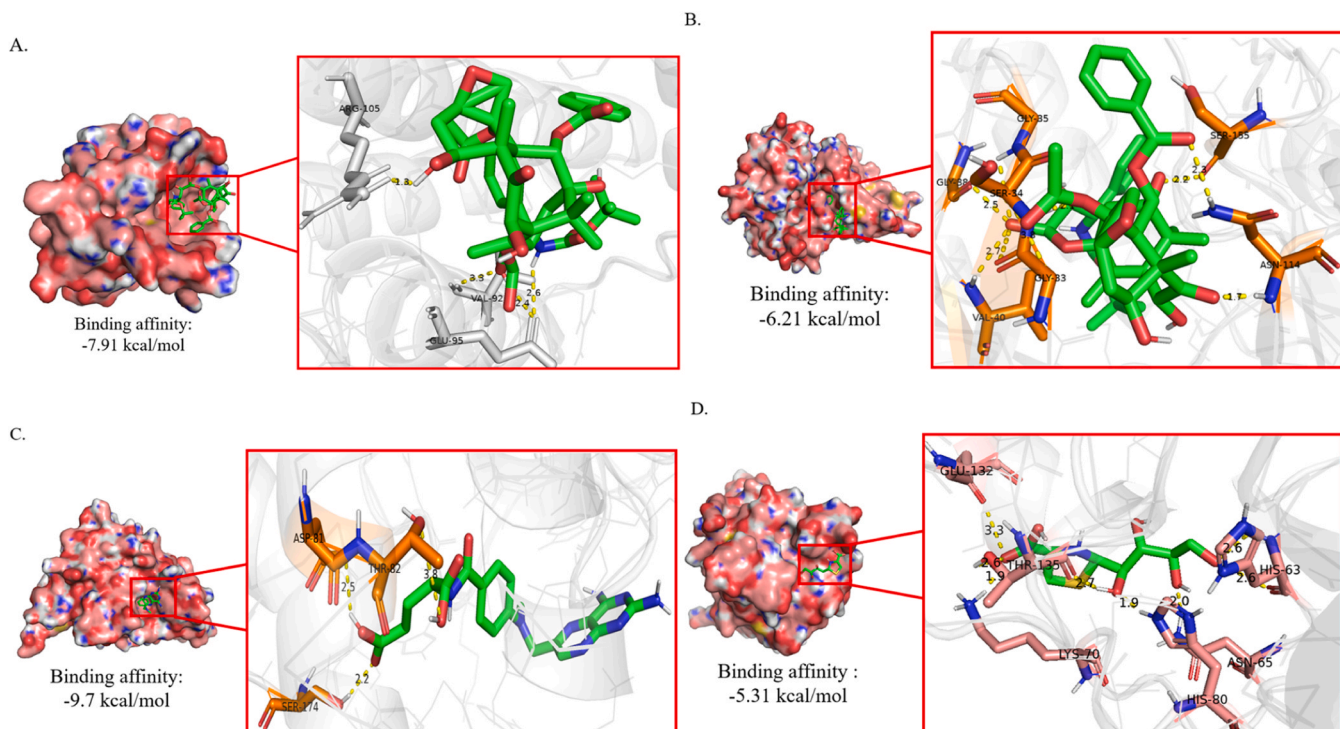


**Fig. 6.** Molecular docking interactions between key therapeutic compounds and core protein targets. (A) Docking of docetaxel (DOC) with BCL2, showing hydrogen bond interactions at ARG-105, GLU-95, and VAL-92. (B) Docking of DOC with MAPK8, forming hydrogen bonds with residues including LYS-70, HIS-80, ASN-65, HIS-63, THR-135, and GLU-132. (C) Methotrexate (MET) interaction with folate receptor 1 (FOLR1), exhibiting strong binding through hydrogen bonds with ASP-81, THR-82, and SER-174. (D) Docking of riboceine (RIB) with superoxide dismutase (SOD), demonstrating binding via hydrogen bonds with LYS-70, HIS-80, ASN-65, HIS-63, THR-135, and GLU-132. All docking poses were visualized using PyMOL, with binding energies indicating favorable interactions.

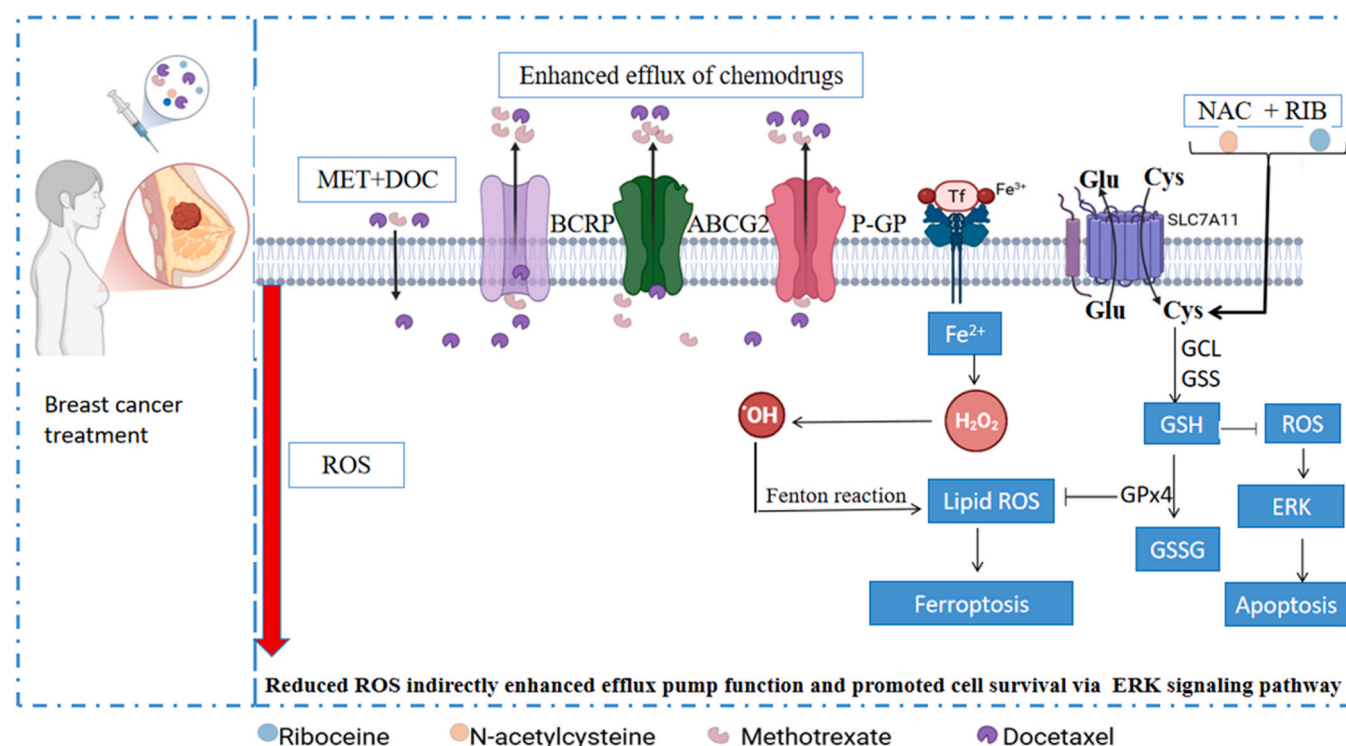


**Fig. 7.** Proposed Mechanism of Antioxidant-Mediated Modulation of Chemotherapy Response and Drug Efflux in Breast Cancer Cells. Schematic illustration of how N-acetylcysteine (NAC) and Ribocaine (RIB) modulate methotrexate (MET) and docetaxel (DOC) activity in chemoresistant breast cancer cells. MET and DOC induce ROS-mediated cytotoxicity, but efflux transporters (e.g., BCRP, ABCG2, P-GP) reduce drug accumulation. NAC and RIB enhance cysteine uptake via SLC7A11, driving glutathione (GSH) synthesis through GCL and GSS. Elevated GSH scavenges ROS, inhibits ferroptosis, and may suppress apoptosis through ERK pathway modulation. This antioxidant response may unintentionally promote drug efflux and cancer cell survival.

drug efficacy in the prostate cancer context. Furthermore, co-treatment of PC3 cells with MET and RIB led to a further reduction in ROS, indicating that the concentration used was sufficient to attenuate oxidative stress without interfering with therapeutic outcomes. In contrast, MET combined with NAC in PC3 cells did not significantly reduce ROS levels compared to MET treatment alone, potentially reflecting dose- or transporter-mediated limitations in intracellular NAC availability.

Although RIB and NAC did not significantly impair the short-term cytotoxic effects of MET and DOC in PC3 cells, their antioxidant activity (evidenced by reduced ROS and restored GSH) still raises concerns about potential long-term consequences. Chronic co-administration of antioxidants may promote adaptive chemoresistance by dampening oxidative stress-mediated apoptosis and activating cytoprotective pathways such as NRF2 or PI3K/Akt. Indeed, several studies have reported that persistent antioxidant exposure can enhance survival signaling and reduce drug sensitivity over time in various cancer types [63,64]. Future studies should therefore investigate the effects of prolonged or repeated antioxidant exposure on drug sensitivity and resistance development in cancer cells initially responsive to chemotherapy.

In MCF-7 cells, both RIB and NAC reduced ROS levels but impaired the cytotoxicity of MET and DOC. This finding aligns with previous reports that antioxidants can attenuate chemotherapy efficacy in certain resistant cancer types [65]. Furthermore, previous studies have shown that MCF-7 possesses upregulated levels of amino acid transporters such as SLC7A11, which facilitates intracellular cysteine uptake, thereby enhancing GSH synthesis, lowering oxidative stress, and supporting treatment resistance and cancer proliferation [66]. Future studies could explore the use of lower concentrations or delayed administration of NAC or RIB in MCF-7 chemotherapy protocols, to strike a balance between normal cell protection and sustained anticancer activity.

Cellular viability and drug sensitivity involve complex regulatory networks beyond ROS and GSH alone, including apoptosis signaling

pathways (e.g., caspase-3 activation, Bcl-2 family protein interactions), mitochondrial dynamics, and redox-sensitive pathways such as mitogen-activated protein kinase (MAPK), phosphoinositide 3-kinase/Akt (PI3K/Akt), and nuclear factor kappa B (NF- $\kappa$ B) signaling cascades [67–70]. Moreover, drug transporter proteins, including breast cancer resistance protein (BCRP) and multidrug resistance-associated proteins (MRPs), which significantly affect chemotherapy efficacy by regulating drug efflux, are also sensitive to redox modulation [71,72]. These redox-sensitive pathways are often activated as part of cellular adaptation to oxidative stress and may contribute to chemoresistance, especially under prolonged antioxidant exposure. Therefore, the observed cytoprotective effects may reflect broader alterations in these molecular pathways.

Although mechanistic assays were not performed in this study, we addressed this limitation by employing a systems biology approach combining network pharmacology and molecular docking to identify potential targets and signaling cascades through which the chemotherapeutic agents and antioxidants may modulate oxidative stress in prostate and breast cancer. From an extensive dataset, 28 common targets were identified across prostate cancer, oxidative stress, and anticancer agents, which also overlapped with targets in breast cancer. Notably, DOC was the only chemotherapeutic agent associated with all 28 targets, highlighting its broad target spectrum and potential as a central modulator in cancer-related oxidative stress. This aligns with studies reporting that DOC is effective in treating various cancers, including prostate cancer [71,72]. In contrast, MET shared only one of these targets, suggesting a more specific mechanism of action. Its selective activity supports its use in metronomic chemotherapy regimens designed to minimize toxicity while maintaining anticancer activity [73].

Antioxidants such as NAC demonstrated overlapping targets with both cancer types and oxidative stress, supporting their potential adjunctive role in mitigating drug-induced oxidative damage. However,

these same targets are involved in cellular survival and stress adaptation, raising concerns about possible interference with drug action depending on timing and dosage. This aligns with previous studies reporting that while NAC may alleviate chemotherapy-induced toxicity, it could also reduce drug efficacy if co-administered simultaneously [74]. Notably, delayed administration (e.g., 4 h post-chemotherapy) may optimize the therapeutic index. In addition, several studies have highlighted that NAC may also exert direct antitumor or anti-proliferative effects depending on the tumor context and redox state, further complicating its dualistic role in cancer therapy [75].

The PPI network analysis further refined these findings by identifying 22 high-confidence intersecting targets, among which 10 hub proteins (e.g., Bcl-2, MAPK8, TNF, EGFR) were prioritized based on maximum clique centralities (MCC) and network topology. These proteins are well-established regulators of apoptosis, inflammation, and oxidative stress, corroborating their relevance in cancer progression and therapy response. Recent studies have reported the use of degree and MCC with shortest path in the CytoHubba plugin to identify targets of significance in biological networks [75,76].

The Bcl-2 family includes both pro-apoptotic and anti-apoptotic members that regulate mitochondrial integrity and caspase activation. Overexpression of pro-survival Bcl-2 proteins or downregulation of pro-apoptotic members has been strongly implicated in the persistence and drug resistance of various cancers [77]. Specifically, the Bcl-2 anti-apoptotic protein is enriched in advanced prostate cancer and facilitates the transition from androgen-dependent to androgen-independent tumor growth, which underpins therapy resistance [78].

The mitogen-activated protein kinase 8 (MAPK8), also known as JNK1, is a member of the MAP kinase family encoded by the MAPK8 gene and is involved in a wide variety of cellular processes such as proliferation, differentiation, transcriptional regulation, and stress responses [79]. MAPK8 activation has been linked to oxidative stress-induced apoptosis, but its inhibition has been shown to enhance chemosensitivity in prostate cancer, likely by blocking pro-survival stress signaling [80].

The tumour necrosis factor (TNF) is a pleiotropic cytokine that plays a dual role in tumor progression and suppression. It is frequently elevated in chronic inflammatory states, including advanced prostate cancer [81]. Although increased levels of TNF can exert apoptotic effects through receptor-mediated caspase activation, chronic exposure often shifts TNF signaling toward nuclear factor-kappa B (NF- $\kappa$ B) activation, which supports tumor growth, angiogenesis, and metastasis, particularly in the presence of other inflammatory mediators such as IL-6 [82].

The epidermal growth factor receptor (EGFR) is a transmembrane receptor tyrosine kinase encoded by a gene located on chromosome 7p12. EGFR plays critical roles in regulating cell growth, proliferation, and survival. Previous studies have shown that interaction of signaling molecules with EGFR activates downstream cascades including PI3K/AKT and RAS/MAPK (ERK), which are frequently dysregulated in cancer and contribute to resistance against chemotherapeutic agents [83]. Aberrant EGFR signaling also promotes epithelial-to-mesenchymal transition (EMT), stemness, and evasion of apoptosis, making it a key therapeutic target in several malignancies, including prostate and breast cancers [84].

Functional enrichment via KEGG analyses revealed significant involvement of the identified targets in cancer-related and stress-responsive signaling pathways, with prostate cancer among the top 20 enriched pathways, whereas breast cancer was notably absent, suggesting distinct molecular modulation profiles in these cancers. This enrichment pattern supports the hypothesis that DOC could modulate PI3K-Akt, MAPK, and p53 signaling pathways (three key regulatory axes involved in cell proliferation, survival, and DNA repair) specifically in prostate cancer. This aligns with several studies that reported efficient cytotoxic activity of DOC in combinational therapy via PI3K-Akt signaling pathways against prostate cancer [85,86]. Moreover, DOC has been reported to induce phosphorylation of MAPK family members,

which in turn regulate redox-sensitive gene transcription and apoptosis-related proteins [87].

GO analysis further emphasized stress-responsive biological processes, such as MAPK signaling cascades and response to reactive oxygen species, reinforcing the notion that DOC can target the interplay between oxidative stress and cancer pathology. This confirms studies that reported that DOC contributed to the surge of oxidative stress in combined therapy against prostate cancer [82]. However, it is critical to note that these predicted pathways and their roles remain putative in this study, as they were not experimentally validated using standard molecular techniques such as ELISA, qPCR, or Western blotting. This lack of validation represents a key limitation, as the expression levels and activity status of predicted targets remain unverified under experimental conditions.

Molecular docking analysis provided further validation of the predicted interactions, with notably strong binding affinities between DOC and key apoptosis-related targets such as BCL2 and MAPK8, as well as favorable binding of MET to the folate receptor FOLR1. The formation of multiple hydrogen bonds and electrostatic interactions in these complexes indicates favorable conformations, suggesting potential inhibition or modulation of these targets under therapeutic conditions. Similarly, the antioxidant RIB showed good binding affinity for superoxide dismutase (SOD), a key enzymatic defense against oxidative damage, while NAC displayed interactions with protein tyrosine phosphatase non-receptor type 1 (PTPN1), further supporting their potential role in mitigating oxidative stress in cancer cells. Nevertheless, these docking results are predictive and should be interpreted with caution pending biochemical validation in future studies.

DOC is a semisynthetic compound derived from taxane that disrupts microtubule dynamics and is widely used as a first-line treatment for metastatic castration-resistant prostate cancer [82,88]. DOC has been shown to interact with BRCA2 at residues GLU and ASP in breast cancer cells [89]. However, in this study, molecular docking predicted alternative interaction profiles, where DOC formed strong binding interactions with apoptosis-related targets such as BCL2 (at residues ARG-105, GLU-95, and VAL-92) and MAPK8 (at residues LYS-70, HIS-80, ASN-65, HIS-63, THR-135, and GLU-132) in prostate cancer cells.

MET, a folic acid analog and antimetabolite originally derived from aminopterin, exerts cytotoxic and immunosuppressive effects by inhibiting dihydrofolate reductase (DHFR), thereby impairing DNA synthesis and repair [90]. MET has been reported to show high binding affinity for human DHFR [91]. In our docking analysis, MET also demonstrated strong affinity for folate receptor alpha (FOLR1), a protein highly expressed in various cancers, including ovarian, breast, and some prostate cancers [92].

RIB (D-ribose-L-cysteine) is a synthetic precursor of cysteine designed to boost intracellular glutathione (GSH) levels and counter oxidative damage [93]. In this study, RIB was predicted to interact favorably with superoxide dismutase (SOD), an enzyme that catalyzes the dismutation of superoxide radicals and serves as a crucial antioxidant defense in both normal and cancer cells.

NAC is a well-characterized thiol-containing compound with established antioxidant, anti-inflammatory, and anti-proliferative properties [94,95]. Docking studies indicated that NAC binds with moderate affinity to protein tyrosine phosphatase non-receptor type 1 (PTPN1), with a binding energy of  $-4.4$  kcal/mol, suggesting possible modulation of redox-sensitive phosphatase activity. While previous studies have demonstrated NAC binding to serum proteins such as bovine serum albumin (BSA), the functional implications of these interactions remain to be experimentally confirmed [96].

Taken together, this integrative bioinformatics approach highlights key molecular targets relevant to prostate cancer and oxidative stress, and supports the potential of combining RIB or NAC with standard chemotherapeutics to enhance therapeutic efficacy while minimizing off-target toxicity. However, these predicted interactions must be interpreted cautiously and validated in future experimental studies.

#### 4.1. Limitations and perspectives

This study highlights the potential of RIB and NAC to reduce chemotherapy-induced toxicity in normal cells while maintaining anti-cancer efficacy against prostate cancer cells. However, several important limitations must be considered before translating these findings into clinical practice.

First, although our study included concentration-response assessments for the chemotherapeutic agents (MET and DOC), we used fixed concentrations of the antioxidants RIB and NAC without a full antioxidant dose- or time-response characterization. Future research should incorporate detailed dose-ranging studies and temporal analyses to determine whether alternative concentrations, delayed administration, or sequential treatment regimens could offer enhanced selectivity, protecting normal cells while preserving cytotoxicity against cancer cells, especially in resistant subtypes such as MCF-7.

Secondly, the study did not directly investigate whether the protective effects of RIB/NAC are mediated via NRF2 activation, a critical redox-sensitive transcription factor. While NRF2 involvement was inferred from GSH restoration and supported by network pharmacology predictions, no protein- or gene-level assays (e.g., qPCR, Western blotting) were performed. Assessing NRF2 expression and pathway activation (using luciferase or immunocytochemistry), as well as its downstream targets, such as HO-1, NQO1, or GCLM, would be essential in elucidating the mechanistic basis of antioxidant activity.

Similarly, NAC and RIB may modulate mitochondrial function, which plays a central role in maintaining redox homeostasis and regulating intrinsic apoptotic signaling. However, key mitochondrial endpoints, including mitochondrial membrane potential ( $\Delta\psi_m$ ), cytochrome c release, and oxidative phosphorylation activity, were not assessed in this study. Future investigations should incorporate assays such as the JC-1 dye assay to evaluate changes in  $\Delta\psi_m$ , which would provide insights into sub-lethal mitochondrial stress and early apoptotic events. These analyses could help elucidate whether mitochondrial signaling pathways contribute to the cell-type-specific cytoprotective or cytotoxic effects observed with antioxidant and chemotherapy co-treatment.

Additionally, cellular uptake and metabolism of antioxidants may differ between cancer cell lines. For example, the SLC7A11 cystine/glutamate antiporter (upregulated in MCF-7 cells) promotes intracellular cysteine accumulation and GSH biosynthesis, supporting drug resistance. Differential expression of related enzymes such as  $\gamma$ -glutamylcysteine synthetase ( $\gamma$ -GCS) may also influence outcomes and should be assessed in future studies. RIB may exert additional antioxidant effects through alternative pathways such as the thioredoxin or peroxiredoxin systems, which remain unexplored in this study.

Another notable limitation is the reliance on two-dimensional (2D) monolayer cell cultures, which do not fully represent the tumor micro-environment's structural complexity, cell-cell interactions, and spatial gradients. As such, our model lacks immune components and pharmacokinetic influences, limiting clinical extrapolation. To bridge this gap, future studies should employ 3D spheroid cultures, tumor organoids, or *in vivo* models (e.g., prostate or breast cancer xenografts). These models would better simulate drug-antioxidant interactions and assess long-term outcomes such as chemoresistance or off-target toxicity.

The study was limited to three cell lines (PNT-2, PC3, MCF-7), which restricts generalizability across cancer types. Expanding to additional cell lines, especially chemoresistant or stem-like subtypes, would enhance translational relevance. Time-course studies are also warranted to capture the dynamic effects of antioxidant intervention over extended periods, including apoptosis progression and recovery.

To differentiate between antioxidant-mediated protection and delayed cytotoxicity, additional apoptosis-specific assays, such as Annexin V/PI staining, caspase-3 activity, or Bax/Bcl-2 ratio analysis, should be integrated in future protocols. These assays would allow more precise characterization of cell death pathways.

Finally, while this study integrated network pharmacology and molecular docking to predict relevant pathways and targets modulated by RIB, NAC, MET, and DOC, these computational insights require empirical validation. Experimental confirmation of predicted targets (e.g., BCL-2, MAPK8, SOD, PTPN1, EGFR) using biochemical approaches such as Western blotting, ELISA, siRNA knockdown, or CRISPR/Cas9 gene editing is necessary to strengthen the causal interpretations. Moreover, signaling cascades identified through KEGG and GO analysis, such as PI3K/Akt, MAPK, and p53 pathways, should be validated using pathway-specific assays to confirm their functional involvement. These follow-up studies will be critical for advancing antioxidant-chemotherapy co-treatment strategies from bench to bedside.

#### 5. Conclusion

This study provides compelling evidence that riboceine (RIB) and N-acetylcysteine (NAC) offer significant cytoprotective effects against the cytotoxic activities of methotrexate (MET) and docetaxel (DOC) in normal prostate epithelial cells (PNT-2). Both antioxidants effectively reduced ROS levels and restored GSH content, mitigating oxidative damage induced by these chemotherapeutic agents. Importantly, these protective effects did not compromise the cytotoxic efficacy of MET and DOC on the PC3 prostate cancer cells, highlighting their selective potential in protecting normal cells without impairing the targeting of cancer cells. In contrast, MCF-7 breast cancer cells exhibited resistance to MET and DOC, likely due to the overexpression of drug efflux proteins and altered microtubule-associated pathways. Co-treatment with RIB or NAC reduced ROS levels and GSH depletion in MCF-7 cells but also impaired the cytotoxic efficacy of MET and DOC, suggesting that antioxidant supplementation may interfere with chemotherapy in certain cancer types. These findings highlight the complexity of antioxidant-chemotherapy interactions and underscore the importance of carefully considering cancer-specific characteristics when employing antioxidant adjunct therapies. Network pharmacology revealed MAPK, PI3K/AKT and p53 signaling pathways to be prominent in modulating prostate cancer. The molecular docking algorithm showed strong binding affinity between DOC-BCL2 and DOC-MAPK8 compound-target pairs.

#### Clinical implications

The selective cytoprotection offered by RIB and NAC supports their potential as adjunct therapies to reduce chemotherapy-induced toxicity in prostate cancer treatment. However, the observed attenuation of cytotoxicity in resistant MCF-7 breast cancer cells cautions against generalized use across all cancer types. Clinicians should consider tumor-specific resistance mechanisms and redox profiles before incorporating antioxidants into chemotherapeutic regimens. Furthermore, timing of administration, for instance, introducing antioxidants several hours after chemotherapy, may help minimize interference with drug efficacy while preserving normal tissue protection. These findings underscore the need for clinical protocols that are tailored to both the tumor biology and the pharmacodynamics of combined treatments.

#### CRedit authorship contribution statement

**Trudy J. Philips:** Writing – original draft, Methodology, Investigation, Formal analysis, Data curation. **N'guessan Benoit Banga:** Writing – review & editing, Writing – original draft, Visualization, Validation, Supervision, Project administration, Methodology, Formal analysis, Data curation, Conceptualization. **Eunice Dotse:** Writing – original draft, Methodology, Investigation. **Joseph Kofi Abankwah:** Writing – original draft, Methodology, Investigation. **Regina Appiah-Opong:** Writing – review & editing, Validation, Supervision, Methodology, Data curation.

## Ethics statement

Protocol for this research was reviewed and approved by the Ethical and Protocol Review Committee of the College of Health Sciences, University of Ghana (Protocol Identification Number: CHS-Et/M.11-P2.10/2017–2018).

## Funding

This research did not receive any specific grant from funding agencies in the public, commercial, or not-for-profit sectors.

## Declaration of Competing Interest

None.

## Acknowledgements

The authors are grateful to the staff of the Department of Clinical Pathology, Noguchi Memorial Institute for Medical Research, College of Health Sciences, University of Ghana, for their support in carrying out this study.

## Data availability

Data will be made available on request.

## References

- Williams, L. Allen, K. Wickramasinghe, B. Mikkelsen, N. Roberts, et al., A Systematic review of associations between non-communicable diseases and socioeconomic status within low- and lower-middle-income countries, *J. Glob. Health* 8 (2) (2018) 020409, <https://doi.org/10.7189/JOGH.08.020409>.
- Z. Wu, F. Xia, R. Lin, Global burden of cancer and associated risk factors in 204 countries and territories, 1980–2021: a systematic analysis for the GBD 2021, *J. Hematol. Oncol.* 17 (119) (2024), <https://doi.org/10.1186/S13045-024-01640-8>.
- F. Bray, M. Laversanne, H. Sung, J. Ferlay, R.L. Siegel, et al., Global cancer statistics 2022: GLOBOCAN estimates of incidence and mortality worldwide for 36 cancers in 185 countries, *CA Cancer J. Clin.* 74 (3) (2024) 229–263, <https://doi.org/10.3322/CAAC.21834>.
- C.M.C. Andrés, J.M. de la Lastra, E.B. Munguira, C.A. Juan, E. Pérez-Lebeña, Dual-action therapeutics: DNA alkylation and antimicrobial peptides for cancer therapy, *Cancers* 16 (18) (2024) 3123, <https://doi.org/10.3390/CANCERS16183123>.
- H. Yang, R.M. Villani, H. Wang, M.J. Simpson, M.S. Roberts, et al., The role of cellular reactive oxygen species in cancer chemotherapy, *J. Exp. Clin. Cancer Res* 37 (1) (2018) 266, <https://doi.org/10.1186/S13046-018-0909-X>.
- H. Nakamura, K. Takada, Reactive oxygen species in cancer: current findings and future directions, *Cancer Sci.* 112 (10) (2021) 3945–3952, <https://doi.org/10.1111/CAS.15068>.
- S.J. Kim, H.S. Kim, Y.R. Seo, Understanding of ROS-inducing strategy in anticancer therapy, *Oxid. Med Cell Longev.* 2019 (1) (2019) 5381692, <https://doi.org/10.1155/2019/5381692>.
- W.M.C. van den Boogaard, D.S.J. Komninos, W.P. Vermeij, Chemotherapy side-effects: not all DNA damage is equal, *Cancers* 14 (3) (2022) 627, <https://doi.org/10.3390/CANCERS14030627>.
- T.W. Mudd, A.K. Guddati, Management of hepatotoxicity of chemotherapy and targeted agents, *Am. J. Cancer Res* 11 (7) (2021) 3461–3474. (<https://pmc.ncbi.nlm.nih.gov/articles/PMC8332851>).
- K. Nurgali, R.T. Jagoe, R. Abalo, Editorial: adverse effects of cancer chemotherapy: anything new to improve tolerance and reduce sequelae, *Front Pharm.* 9 (2018) 245, <https://doi.org/10.3389/FPHAR.2018.00245>.
- J. Zeien, W. Qiu, M. Triay, H.A. Dhaibar, D. Cruz-Topete, et al., Clinical implications of chemotherapeutic agent organ toxicity on perioperative care, *Biomed. Pharm.* 146 (2022) 112503, <https://doi.org/10.1016/j.biopha.2021.112503>.
- K. Jakubczyk, K. Dec, J. Kaiduńska, D. Kawczuga, J. Kochman, et al., Reactive oxygen species - sources, functions, oxidative damage, *Pol. Merkur Lek.* 48 (284) (2020) 124–127. (<https://europepmc.org/article/med/32352946>).
- M. Schieber, N.S. Chandel, ROS function in redox signaling and oxidative stress, *Curr. Biol.* 24 (10) (2014) R453–R462, <https://doi.org/10.1016/j.CUB.2014.03.034>.
- M.A. Shah, H.A. Rogoff, Implications of reactive oxygen species on cancer formation and its treatment, *Semin Oncol.* 48 (3) (2021) 238–245, <https://doi.org/10.1053/J.SEMINONCOL.2021.05.002>.
- N. Chandimali, S.G. Bak, E.H. Park, H.J. Lim, Y.S. Won, et al., Free radicals and their impact on health and antioxidant defenses: a review, *Cell Death Discov.* 11 (1) (2025) 1–17, <https://doi.org/10.1038/s41420-024-02278-8>.
- A.B. Jena, R.R. Samal, N.K. Bhol, A.K. Duttaroy, Cellular red-ox system in health and disease: the latest update, *Biomed. Pharm.* 162 (2023) 114606, <https://doi.org/10.1016/j.biopha.2023.114606>.
- K. Jomova, R. Raptova, S.Y. Alomar, S.H. Alwasel, E. Nepovimova, et al., Reactive Oxygen Species, Toxicity, Oxidative Stress, and Antioxidants: Chronic Diseases and Aging, *Arch. Toxicol.* 97 (10) (2023) 2499–2574, <https://doi.org/10.1007/S00204-023-03562-9>.
- K. Jomova, S.Y. Alomar, S.H. Alwasel, E. Nepovimova, K. Kuca, et al., Several lines of antioxidant defense against oxidative stress: antioxidant enzymes, nanomaterials with multiple enzyme-mimicking activities, and low-molecular-weight antioxidants, *Arch. Toxicol.* 98 (5) (2024) 1323–1367, <https://doi.org/10.1007/S00204-024-03696-4>.
- B. Poljsak, D. Suptut, I. Milisav, Achieving the balance between ROS and antioxidants: when to use the synthetic antioxidants, *Oxid. Med Cell Longev.* 2013 (1) (2013) 956792, <https://doi.org/10.1155/2013/956792>.
- X. An, W. Yu, J. Liu, D. Tang, L. Yang, et al., Oxidative cell death in cancer: mechanisms and therapeutic opportunities, *Cell Death Dis.* 15 (8) (2024) 1–20, <https://doi.org/10.1038/s41419-024-06939-5>.
- H.J. Forman, H. Zhang, A. Rinna, Glutathione: overview of its protective roles, measurement, and biosynthesis, *Mol. Asp. Med* 30 (1-2) (2009) 1–12, <https://doi.org/10.1016/J.MAM.2008.08.006>.
- S.K. Georgiou-Siafis, A.S. Tsiftoglou, The key role of GSH in keeping the redox balance in mammalian cells: mechanisms and significance of GSH in detoxification via formation of conjugates, *Antioxidants* 12 (11) (2023) 1953, <https://doi.org/10.3390/ANTIOX12111953>.
- L. Kennedy, J.K. Sandhu, M.E. Harper, M. Cuperlovic-culf, Role of glutathione in cancer: from mechanisms to therapies, *Biomolecules* 10 (10) (2020) 1–27, <https://doi.org/10.3390/B10101429>.
- V.I. Lushchak, Glutathione homeostasis and functions: potential targets for medical interventions, *J. Amino Acids* 2012 (2012) 1–26, <https://doi.org/10.1155/2012/736837>.
- N. Traverso, R. Ricciarelli, M. Nitti, B. Marengo, A.L. Furfaro, et al., Role of glutathione in cancer progression and chemoresistance, *Oxid. Med Cell Longev.* 2013 (1) (2013) 972913, <https://doi.org/10.1155/2013/972913>.
- A.E. Saltman, D-Ribose-L-cysteine supplementation enhances wound healing in a rodent model, *Am. J. Surg.* 210 (1) (2015) 153–158, <https://doi.org/10.1016/J.AMJSURG.2014.11.014>.
- C. Kerksick, D. Willoughby, The antioxidant role of glutathione and N-acetyl-cysteine supplements and exercise-induced oxidative stress, *J. Int. Soc. Sports Nutr.* 2 (2) (2005) 38–44, <https://doi.org/10.1186/1550-2783-2-2-38>.
- K.R. Atkuri, J.J. Mantovani, L.A. Herzenberg, L.A. Herzenberg, N-acetylcysteine-a safe antidote for cysteine/glutathione deficiency, *Curr. Opin. Pharm.* 7 (4) (2007) 355–359, <https://doi.org/10.1016/J.COPH.2007.04.005>.
- G.T. Akingbade, O.M. Ijomone, A. Imam, M. Aschner, M.S. Ajao, D-ribose L-cysteine attenuates manganese-induced cognitive and motor deficit, oxidative damage, and reactive microglia activation, *Environ. Toxicol. Pharm.* 93 (2022) 103872, <https://doi.org/10.1016/J.ETAP.2022.103872>.
- H.J. Forman, H. Zhang, Targeting oxidative stress in disease: promise and limitations of antioxidant therapy, *Nat. Rev. Drug Discov.* 20 (9) (2021) 689–709.
- B. Poljsak, I. Milisav, The role of antioxidants in cancer, friends or foes? *Curr. Pharm. Des.* 1;24 (44) (2018) 5234–5244.
- D. Trachootham, J. Alexandre, P. Huang, Targeting cancer cells by ROS-mediated mechanisms: a radical therapeutic approach? *Nat. Rev. Drug Discov.* 8 (7) (2009) 579–591.
- S.C. Lu, Regulation of glutathione synthesis, *Mol. Asp. Med.* 30 (1-2) (2009) 42–59.
- M. Dean, A. Rzhetsky, R. Allikmets, The human ATP-binding cassette (ABC) transporter superfamily, *Genome Res* 11 (7) (2001) 1156–1166, <https://doi.org/10.1101/gr.184901>.
- E. Di Zazzo, G. Galasso, P. Giovannelli, M. Di Donato, A. Di Santi, G. Cernaia, V. Rossi, C. Abbonanza, B. Monchamont, A.A. Sinisi, G. Castoria, A. Migliaccio, Prostate cancer stem cells: the role of androgen and estrogen receptors, *Oncotarget* 7 (1) (2016) 193–208, <https://doi.org/10.18632/oncotarget.6220>.
- K.A. Conklin, Chemotherapy-associated oxidative stress: impact on chemotherapeutic effectiveness, *Integr. Cancer Ther.* 3 (4) (2004) 294–300, <https://doi.org/10.1177/1534735404270335>.
- A. Ghoneum, A.Y. Abdulfattah, B.O. Warren, J. Shu, N. Said, Redox homeostasis and metabolism in cancer: a complex mechanism and potential targeted therapeutics, *Int. J. Mol. Sci.* 21 (9) (2020) 3100, <https://doi.org/10.3390/ijms21093100>.
- E. Tsakalozou, A.M. Eckman, Y. Bae, Combination effects of docetaxel and doxorubicin in hormone-refractory prostate cancer cells, *Biochem Res Int* 2012 (2012) 832059, <https://doi.org/10.1155/2012/832059>.
- G. Muñoz-Sánchez, L.A. Godínez-Méndez, M. Fafutis-Morris, V. Delgado-Rizo, Effect of antioxidant supplementation on NET formation induced by LPS in vitro: the roles of vitamins E and C, glutathione, and N-acetyl cysteine, *Int. J. Mol. Sci.* 24 (17) (2023 Aug 24) 13162, <https://doi.org/10.3390/ijms241713162>.
- S. Mulè, S. Ferrari, G. Rosso, A. Brovero, M. Botta, A. Congiusta, R. Galla, C. Molinari, F. Uberty, The combined antioxidant effects of N-acetylcysteine, vitamin D3, and glutathione from the intestinal-neuronal in vitro model, *Foods* 13 (5) (2024 Mar 1) 774, <https://doi.org/10.3390/foods13050774>.
- Finnerty M.C., Leach I.L.I.F.E., Zakharia Y., Nepple K.G., Bartlett M.G., et al. Identification of blood lipid markers of docetaxel treatment in prostate cancer patients. *Scientific reports* 2024; 14(1): 22069, doi: 10.1038/s41598-024-73074-8.
- M.A. Martin, S. Ramos, R. Mateos, A.B. Granado Serrano, M. Izquierdo-Pulido, et al., Protection of human Hepg2 cells against oxidative stress by cocoa phenolic extract, *J. Agric. Food Chem.* 56 (17) (2008) 7765–7772, <https://doi.org/10.1021/JF801744R>.

- [43] A. Kawiak, J. Zawacka-Pankau, A. Wasilewska, G. Stasioljc, J. Bigda, et al., Induction of apoptosis in HL-60 cells through the ros-mediated mitochondrial pathway by ramentacene from *Drosera aliciae*, *J. Nat. Prod.* 75 (1) (2012) 9–14, <https://doi.org/10.1021/NP200247G>.
- [44] H. Ying, W. Kong, X. Xu, Integrated network pharmacology, machine learning and experimental validation to identify the key targets and compounds of tiaoshengongjian for the treatment of breast cancer, *Onco Targets Ther.* 18 (2025) 49, <https://doi.org/10.2147/OTT.S486300>.
- [45] H. Hozhabri, R.S. Ghasemi Dehkohneh, S.M. Razavi, S.M. Razavi, F. Salarian, et al., Comparative analysis of protein-protein interaction networks in metastatic breast cancer, *PLoS One* 17 (1) (2022) e0260584, <https://doi.org/10.1371/JOURNAL.PONE.0260584>.
- [46] T. Sang, T. Zhang, J. Wang, Y. Zheng, Network pharmacology and molecular docking analysis on molecular targets and mechanisms of bushen hugu decoction in the treatment of malignant tumor bone metastases, *Biomed. Res Int* 2022 (2022) 2055900, <https://doi.org/10.1155/2022/2055900>.
- [47] C. Wen-Tao, Y.Y. Zhang, Q. Qiang, P. Zou, Y. Xu, et al., Characterizations and molecular docking mechanism of the interactions between peptide FDGDF (phe-Asp-Gly-Asp-Phe) and SOD enzyme, *Heliyon* 10 (2) (2024) E24515, <https://doi.org/10.1016/J.HELIYON.2024.E24515>.
- [48] D. Kolodziej-Sobczak, Sobczak Ł, Płaziński W, Sławińska-Brych A, Mizerska-Kowalska M, et al. Design, synthesis, molecular docking and anticancer activity evaluation of methyl salicylate-based thiazoles as PTP1B inhibitors, *Sci. Rep.* 15 (1) (2025) 1–15, <https://doi.org/10.1038/S41598-025-88038-9>.
- [49] C. Kirubhanand, J. Selvaraj, U.V. Rekha, V. Vishnupriya, V. Sivabalan, et al., Molecular docking analysis of Bcl-2 with phyto-compounds, *Bioinformation* 16 (6) (2020) 468, <https://doi.org/10.6026/97320630016468>.
- [50] J. Li, X. Wang, L. Xue, Q. He, Exploring the therapeutic mechanism of curcumin in prostate cancer using network pharmacology and molecular docking, *Heliyon* 10 (12) (2024) E33103, <https://doi.org/10.1016/J.HELIYON.2024.E33103>.
- [51] A. Troyano, C. Fernández, P. Sancho, E. De Blas, P. Aller, Effect of glutathione depletion on antitumor drug toxicity (apoptosis and necrosis) in U-937 human promonocytic cells: the role of intracellular oxidation, *J. Biol. Chem.* 276 (50) (2001) 47107–47115, <https://doi.org/10.1074/JBC.M104516200>.
- [52] R.F. Alserihi, M.R.S. Mohammed, M. Kaleem, M.I. Khan, M. Sechi, et al., Development of (-)-epigallocatechin-3-gallate-loaded folate receptor-targeted nanoparticles for prostate cancer treatment, *Nanotechnol. Rev.* 11 (1) (2021) 298–311, <https://doi.org/10.1515/NTREV-2022-0013>.
- [53] L. Ippolito, A. Marini, L. Cavallini, A. Morandi, L. Pietrovito, et al., Metabolic shift toward oxidative phosphorylation in docetaxel resistant prostate cancer cells, *Oncotarget* 7 (38) (2016) 61890–61904, <https://doi.org/10.18632/oncotarget.11301>.
- [54] V.I. Sayin, M.X. Ibrahim, E. Larsson, J.A. Nilsson, P. Lindahl, M.O. Bergh, Antioxidants accelerate lung cancer progression in mice, *Sci. Transl. Med.* 6 (221) (2014 Jan 29), 221ra15.
- [55] M. Stapf, N. Pömpner, U. Teichgräber, I. Hilger, Heterogeneous response of different tumor cell lines to methotrexate-coupled nanoparticles in presence of hyperthermia, *Int J. Nanomed.* 11 (2016) 485, <https://doi.org/10.2147/IJN.S94384>.
- [56] C. Wiltshire, B.L. Singh, J. Stockley, J. Fleming, B. Doyle, et al., Docetaxel-resistant prostate cancer cells remain sensitive to S-trityl-L-cysteine-mediated Eg5 inhibition, *Mol. Cancer Ther.* 9 (6) (2010) 1730–1739, <https://doi.org/10.1158/1535-7163.MCT-09-1103>.
- [57] Z. Wang, R. Goulet, K.J. Stanton, M. Sadaria, H. Nakshatri, Differential effect of anti-apoptotic genes Bcl-xL and c-FLIP on sensitivity of MCF-7 breast cancer cells to paclitaxel and docetaxel, *Anticancer Res.* 25 (3C) (2005 May 1) 2367–2379.
- [58] N.O. Sahin, M. Berköz, E.D. Eker, B. Pomierny, K. Przejczowska, Cytotoxic and antioxidant effects of grape seed oil on the treatment of leukemia with methotrexate, *Eur. J. Chem.* 3 (2) (2012) 147–151, <https://doi.org/10.1515/eurjchem.3.2.147-151.569>.
- [59] M. De Nicola, L. Ghibelli, Glutathione depletion in survival and apoptotic pathways, *Front Pharm.* 5 (2014) 267, <https://doi.org/10.3389/fphar.2014.00267>.
- [60] A.R. Moghadam, S. Tutunchi, A. Namvaran-Abbas-Abad, M. Yazdi, F. Bonyadi, et al., Pre-administration of turmeric prevents methotrexate-induced liver toxicity and oxidative stress, *BMC Complement Alter. Med* 15 (1) (2015) 1–13, <https://doi.org/10.1186/S12906-015-0773-6>.
- [61] V.O. Ukwenya, M.O. Alese, B. Ogunlade, I.M. Folorunso, O.I. Omotuyi, *Anacardium occidentale* leaves extract and ribocaine mitigate hyperglycemia through anti-oxidative effects and modulation of some selected genes associated with diabetes, *J. Diabetes Metab. Disord.* 22 (1) (2022) 455, <https://doi.org/10.1007/S40200-022-01165-2>.
- [62] H. Pelicano, D. Carney, P. Huang, ROS stress in cancer cells and therapeutic implications, *Drug Resist Updat* 7 (2) (2004) 97–110, <https://doi.org/10.1016/J.DRUP.2004.01.004>.
- [63] K. Manupati, S. Debnath, K. Goswami, P.S. Bhoj, H.S. Chandak, S.P. Bahekar, A. Das, Glutathione S-transferase omega 1 inhibition activates JNK-mediated apoptotic response in breast cancer stem cells, *FEBS J.* 286 (11) (2019 Jun) 2167–2192.
- [64] L. Kennedy, J.K. Sandhu, M.E. Harper, M. Cuperlovic-Culf, Role of glutathione in cancer: from mechanisms to therapies, *Biomolecules* 10 (10) (2020 Oct 9) 1429.
- [65] A.W.M. Nielsen, M.H. Kristensen, B.V. Offersen, J. Alsner, R. Zachariae, et al., Patient-reported outcomes in postmenopausal breast cancer survivors-comparisons with normative data, *Acta Oncol. (Madr.)* 60 (1) (2021) 78–86, <https://doi.org/10.1080/0284186X.2020.1834143>.
- [66] Y.J. Cha, E.S. Kim, J.S. Koo, Amino acid transporters and glutamine metabolism in breast cancer, *Int J. Mol. Sci.* 19 (3) (2018) 907, <https://doi.org/10.3390/IJMS19030907>.
- [67] M. Redza-Dutordoir, D.A. Averill-Bates, Activation of apoptosis signalling pathways by reactive oxygen species, *Biochimica et Biophysica Acta (BBA) Molecular Cell Research* 1863 (12) (2016) 2977–2992, <https://doi.org/10.1016/j.bbamcr.2016.09.012>.
- [68] B. Perillo, M. Di Donato, A. Pezone, E. Di Zazzo, P. Giovannelli, G. Galasso, G. Castoria, ROS in cancer therapy: the bright side of the moon, *Exp. Mol. Med.* 52 (2) (2020) 192–203, <https://doi.org/10.1038/s12276-020-0384-2>.
- [69] J.N. Moloney, T.G. Cotter, ROS signalling in the biology of cancer, *Semin. Cell Dev. Biol.* 80 (2018) 50–64, <https://doi.org/10.1016/j.semcdb.2017.05.023>.
- [70] C.R. Reczek, N.S. Chandel, The two faces of reactive oxygen species in cancer, *Annu. Rev. Cancer Biol.* 1 (2017) 79–98, <https://doi.org/10.1146/annurev-cancerbio-041916-065808>.
- [71] E. Rivero-Buceta, A. Bernal-Gómez, C. Vidaurre-Agut, E.L. Moncholi, J. M. Benloch, et al., Prostate cancer chemotherapy by intratumoral administration of docetaxel-mesoporous silica nanomedicines, *Int J. Pharm.* (2024) 664, <https://doi.org/10.1016/j.ijpharm.2024.124623>.
- [72] Q.H. Chen, Crosstalk between microtubule stabilizing agents and prostate cancer, *Cancers* 15 (13) (2023) 3308, <https://doi.org/10.3390/cancers15133308>.
- [73] N. Jan, S. Sofi, H. Qayoom, A. Shabir, B.U. Haq, M.A. Macha, et al., Metronomic chemotherapy and drug repurposing: a paradigm shift in oncology, *Heliyon* 10 (3) (2024) e24670, <https://doi.org/10.1016/j.heliyon.2024.e24670>.
- [74] L.L. Muldoon, Y.J. Wu, M.A. Pagel, E.A. Neuwelt, N-acetylcysteine chemoprotection without decreased cisplatin antitumor efficacy in pediatric tumor models, *J. Neurooncol* 121 (3) (2015) 433–440, <https://doi.org/10.1007/S11060-014-1657-1>.
- [75] J. Wang, Z. Zhang, Q. Li, Z. Hu, Y. Chen, et al., Network pharmacology and molecular docking reveal the mechanisms of curcumin activity against esophageal squamous cell carcinoma, *Front Pharm.* 15 (2024) 1282361, <https://doi.org/10.3389/FPHAR.2024.1282361/BIBTEX>.
- [76] X. Tan, Y.P. Du, Q. Luo, X.B. Zhan, Y.S. Kuang, et al., Network pharmacology and molecular docking analysis of the mechanism underlying Yikunyin's therapeutic effect on menopausal syndrome, *J. Evid. Based Complement Alter. Med* 2022 (1) (2022) 7302419, <https://doi.org/10.1155/2022/7302419>.
- [77] D. Kaloni, S.T. Diepstraten, A. Strasser, G.L. Kelly, BCL-2 protein family: attractive targets for cancer therapy, *Apoptosis* 28 (1-2) (2023) 20–38, <https://doi.org/10.1007/S10495-022-01780-7>.
- [78] D. Westaby, J.M. Jiménez-Vacas, I. Figueiredo, J. Rekowski, C. Pettinger, et al., BCL2 expression is enriched in advanced prostate cancer with features of lineage plasticity, *J. Clin. Invest* 134 (18) (2024), <https://doi.org/10.1172/JCI179998>.
- [79] J. Li, X. Wang, L. Xue, Q. He, Exploring the therapeutic mechanism of curcumin in prostate cancer using network pharmacology and molecular docking, *Heliyon* 10 (12) (2024) E33103, <https://doi.org/10.1016/J.HELIYON.2024.E33103>.
- [80] D. Gioelli, J.W. Mandell, G.R. Petroni, H.F. Frierson Jr, M.J. Weber, Activation of mitogen-activated protein kinase associated with prostate cancer progression, *Cancer Res.* 59 (2) (1999 Jan 15) 279–284.
- [81] C. Driscoll, N. Handa, Y. Hao, M. Alshalfá, A.K. Hakansson, et al., Tumor necrosis factor alpha signaling activity and NCCN risk, adverse pathology, and progression during active surveillance in prostate cancer, 415–415, *J. Clin. Oncol.* 43 (5) (2025), [https://doi.org/10.1200/JCO.2025.43.5\\_SUPPL.415](https://doi.org/10.1200/JCO.2025.43.5_SUPPL.415).
- [82] S.A. Fadil, D.A.I. Albadawi, K.Z. Alshali, H.M. Abdallah, M.M. Saber, Modulation of inflammatory mediators underlies the antitumor effect of the combination of morusin and docetaxel on prostate cancer cells, 415–415, *Biomed. Pharm.* 43 (5) (2024), <https://doi.org/10.1016/J.BIOPHA.2024.117572>.
- [83] A.A. Rosenkranz, T.A. Slastnikova, Epidermal growth factor receptor: key to selective intracellular delivery, *Biochemistry (Mosc)* 85 (9) (2020) 967–993, <https://doi.org/10.1134/S000629720090011>.
- [84] S. Halder, S. Basu, S.P. Lall, A.K. Ganti, S.K. Batra, P. Seshacharyulu, Targeting the EGFR signaling pathway in cancer therapy: what's new in 2023? *Expert Opin. Ther. Targets* 27 (4-5) (2023 May 4) 305–324.
- [85] W. Xu, J. Ding, S. Kuang, B. Li, T. Sun, et al., Icarin-curcumin promotes docetaxel sensitivity in prostate cancer through modulation of the PI3K-Akt signaling pathway and the warburg effect, *Cancer Cell Int* 23 (1) (2023) 1–15, <https://doi.org/10.1186/S12935-023-03042-1>.
- [86] A. Dirican, H. Atmaca, E. Bozkurt, C. Erten, B. Karaca, et al., Novel combination of docetaxel and thymoquinone induces synergistic cytotoxicity and apoptosis in du-145 human prostate cancer cells by modulating PI3K-AKT pathway, *Clin. Transl. Oncol.* 17 (2) (2015) 145–151, <https://doi.org/10.1007/S12094-014-1206-6>.
- [87] C. Yang, W. Zhang, J. Wang, P. Chen, J. Jin, Effect of docetaxel on the regulation of proliferation and apoptosis of human prostate cancer cells, *Mol. Med. Rep.* 19 (5) (2019 May) 3864–3870.
- [88] R. Roskoski Jr, Targeted and cytotoxic inhibitors used in the treatment of breast cancer, *Pharm. Res* 210 (2024) 107534, <https://doi.org/10.1016/J.PHRS.2024.107534>.
- [89] M. Genc, Z.K. Genc, S. Tekin, S. Sandal, M. Sirajuddin, et al., Design, synthesis, in vitro antiproliferative activity, binding modeling of 1,2,4-triazoles as new anti-breast cancer agents, *Acta Chim. Slov.* 63 (4) (2016) 726–737, <https://doi.org/10.17344/ACSLS.2016.2428>.
- [90] M. Czarnačka-Operacz, A. Sadowska-Przytocka, The possibilities and principles of methotrexate treatment of psoriasis - the updated knowledge, *Post. Derm. Alergol.* 31 (6) (2014) 392–400, <https://doi.org/10.5114/PDIA.2014.47121>.
- [91] R.M. Rana, S. Rampogu, N.B. Abid, A. Zeb, S. Parate, In silico study identified methotrexate analog as potential inhibitor of drug resistant human dihydrofolate

- reductase for cancer therapeutics, *Molecules* 25 (15) (2020) 3510, <https://doi.org/10.3390/MOLECULES25153510>.
- [92] H.J. Bax, J. Chauhan, C. Stavrika, A. Santaolalla, G. Osborn, et al., Folate receptor alpha in ovarian cancer tissue and patient serum is associated with disease burden and treatment outcomes, *Br. J. Cancer* 128 (2) (2023) 342–353, <https://doi.org/10.1038/S41416-022-02031-X>.
- [93] S.K. Amponsah, B.B. N'guessan, M. Akandawen, A. Aning, S.Y. Agboli, et al., Effect of cellgevity® supplement on selected rat liver cytochrome p450 enzyme activity and pharmacokinetic parameters of carbamazepine, *Evid. Based Complement Altern. Med* 2020 (2020) 7956493, <https://doi.org/10.1155/2020/7956493>.
- [94] J. Chen, Y. Cheng, H. Cui, S. Li, L. Duan, et al., N-Acetyl-L-cysteine protects rat lungs and RLE-6TN cells from cigarette smoke-induced oxidative stress, *Mol. Med Rep.* 31 (4) (2025) 1–10, <https://doi.org/10.3892/mmr.2025.13462>.
- [95] P. Santus, J.C. Signorello, F. Danzo, G. Lazzaroni, M. Saad, et al., Anti-inflammatory and anti-oxidant properties of N-acetylcysteine: a fresh perspective, *J. Clin. Med* 13 (14) (2024) 4127, <https://doi.org/10.3390/JCM13144127>.
- [96] L. Rind, M. Ahmad, M.I. Khan, J. Akhtar, U. Ahmad, et al., An insight on safety, efficacy, and molecular docking study reports Of N-acetylcysteine and its compound formulations, *J. Basic Clin. Physiol. Pharm.* 33 (3) (2022) 223–233, <https://doi.org/10.1515/JBCPP-2020-0099>.